1991

Debris flows and the morphogenesis of hollows near Sunol, Alameda County, California

Christopher Stuart Alger
San Jose State University

Order Number 1347139

Debris flows and the morphogenesis of hollows near Sunol, Alameda County, California

Alger, Christopher Stuart, M.S.

San Jose State University, 1991

U·M·I
300 N. Zeeb Rd.
Ann Arbor, MI 48106

DEBRIS FLOWS AND THE MORPHOGENESIS OF HOLLOWS NEAR SUNOL, ALAMEDA COUNTY, CALIFORNIA

A Thesis

Presented to

The Faculty of the Department of Geology

San Jose State University

In Partial Fulfillment

of the Requirements for the Degree

Master of Science

By

Christopher Stuart Alger

December, 1991

APPROVED FOR THE DEPARTMENT OF GEOLOGY

Dr. John W.Williams

Dr. Stephen D. Ellen

Dr. David W. Andersen

APPROVED FOR THE UNIVERSITY

ACKNOWLEDGEMENTS

I am very grateful to the San Francisco Water Department and their staff at the Sunol Water Temple for allowing me access to their property during this study. In addition, I would like to acknowledge the material and financial support that have been given to me by the U.S. Geological Survey; Rogers Pacific, Professional Engineering Consultants; and McLaren/Hart Environmental Consulting. My research and this thesis has benefitted greatly from the teaching and patient guidance that the members of my thesis committee have provided throughout this long process. I especially thank Steven Ellen for the many hours of time he has devoted to my learning.

As with any project of this nature, this thesis has gained much from the many discussions and arm-waving episodes that I have shared with my friends and coworkers. In particular, I would like to thank Dave Montgomery, Steve Reneau, Dave Rogers, Rob Olshansky, Fausto Guzzetti, Gerry Wieczorek, Rich Baldwin, and Kathleen Isaacson. The graphical presentations in the thesis improved from the help of Lisa Asche and Lorraine Hollis.

This work would not have been possible without the support of my wife Kathleen, and my children Erin and Loryn, who followed many a cow path with me. This thesis is dedicated to my parents, Bob and Marjie Alger, who have always encouraged me to pursue my interests and goals. My thanks.

TABLE OF CONTENTS

Page

ABSTRACT xi

INTRODUCTION 1

PREVIOUS WORK 7

Debris Flows 7

Hollows 9

METHODS 11

SETTING 15

Location 15

Landforms 15

Drainages 18

Hillslopes 18

Planar Slopes 22

Spurs 22

Hollows 22

Stratigraphy 29

Bedrock 29

Colluvial Deposits 31

Soils 34

Structural Geology and Tectonics 35

Climate 35

Page

Vegetation 38

HOLLOW MORPHOLOGY 40

Physical Description 40

Profile Description 44

Zone 1 - Transitional Hollow Lip 47

Zone 2 - Main Hollow 47

Zone 3 - Depositional Area 48

Variations 48

Slope-inclination Inventory 52

DEBRIS FLOW AND OTHER HILLSLOPE PROCESSES IN THE
STUDY AREA 55

Soil Slips and Debris Flows in the Study Area 55

Typical Components 57

Form and Size of Failures 57

Mobilization 57

Flow and Scour 61

Water Flow from Scars 65

Scar Weathering and Revegetation 65

Channel-bank Failures 67

Other Slope Processes 72

Page

SPATIAL RELATIONSHIPS BETWEEN DEBRIS FLOWS AND HOLLOWS 75

Debris-flow Occurrence 75

Area of Hollows 77

GENETIC RELATIONSHIP BETWEEN DEBRIS FLOWS AND HOLLOWS 79

Sufficiency of Debris-flow Processes 79

Approach 79

Volume 80

Erosion Rates 83

Climatic Constraints 87

Continuum of Hollow Size and Continuity of Process 87

HOLLOW INITIATION AND DEVELOPMENT 89

Hollow Initiation 91

Hollow Enlargement 92

CONCLUSIONS 95

REFERENCES CITED 97

APPENDIX I: SOIL PROFILE DESCRIPTIONS 101

LIST OF ILLUSTRATIONS

Figure		Page
1.	Location of Study Area	2
2.	Aerial View of Study Area	3
3.	Debris-flow Scars in Hollow	4
4.	Typical Features of a Soil Slip-Debris Flow	8
5.	Exposure of Deposits from Debris Flows	12
6.	Aerial View Looking to the Northeast	16
7.	Location Map Showing Selected Geomorphic Features	17
8.	View to the East in the Upstream Part of Drainage D1	19
9.	View of Stream Head of Drainage D2	20
10.	Discontinuous Stream Channel in Drainage D3	21
11.	Diagram of Typical Linear Drainage with Planar Slopes Dissected by Hollows	23
12.	Subparallel, Planar Appearance of the Pre-hollow Valley Walls in Drainage D1	24
13.	Spur Ridges between Hollows	25
14.	Gently Sloping Upland Surface and the Sidewalls of Drainage D1	26
15.	Well Developed Hollows and Spurs of Drainage D1	27

Figure | Page

16. The Largest Hollow in the Study Area, Showing the Typical Funnel-shaped Form 28

17. Close-up View of an Outcrop of Cemented Livermore Gravels . . 30

18. Broad, Arcuate Zone of Old Colluvium 32

19. Exposure of Old Colluvium at the Head of Drainage D2 33

20. Aerial Oblique View Looking North up the Sunol Valley 36

21. Uplift along Portion of the Calaveras Fault 37

22. Terracettes are Common on Hillslopes Throughout the Study Area 39

23. Diagram of Typical Hollow Features Showing Terminology Used in Text 41

24. View of One of the Smaller Hollows in the Study Area 42

25. View of a Large, Complex Hollow in Drainage D2 43

26. Diagram of Hollow Geometry Showing Relation of Axial and Plan Curvature to Hollow 45

27. Profiles of Spur and Hollow Axes 46

28. Mouth of a Medium-sized Hollow 49

29. Gully Incision in a Hollow in Drainage D1 50

30. View of a Compound Hollow 51

31. Large Hollow Eroded Back Through Resistant Bedrock Outcrop 53

Figure Page

32. Histograms of Hollow and Spur Inclinations 54

33. Upper Lip of a Hollow in Drainage D1 60

34. Scar and Flow Path of a 1986 Debris Flow 62

35. Close-up View of a Small 1986 Debris-flow Scar and
Flow Path One Week after Failure 63

36. Debris Flows Triggered during 10-day Storm 64

37. Detail of Headscarp of Debris-flow Scar 66

38. Detail of a Weathered Scar Surface 69

39. Cross Section of a Terracette 70

40. View of the Upstream Termination of the Incised
Portion of Drainage D1 71

41. Track of Flushed Debris in Hollow Axis 74

42. Estimate of Hollow Plan Area and Approximate
Volumes of Hollows 82

43. Relationship of Slope Relief to Isolation of Debris-flow Scars . . . 90

44. Impact and Location of Slope Erosion by Debris Flows 93

Plate

1. Map of Selected Geomorphic Features in Study Area ..... in pocket

LIST OF TABLES

Table Page

1. Data on 1986 Debris Flows 56
2. Soil Analytical Data for Sampled Debris Flows 58
3. Aerial Photographs 68
4. Topographic Position of Debris-flow Scars 76
5. Areas and Area Percentages 78
6. 1986 Storm Data 81
7. Volume Calculations 84

ABSTRACT

An uplifted block along the active Calaveras fault near the town of Sunol in the San Francisco Bay area, California, is in the early stages of landscape development, characterized by rejuvenation and incision of the major streams. Incision has been accompanied by the development of non-channelized zero-order basins along the valley slopes of these streams. These zero-order basins are the subject of this study. The non-channelized nature of these basins suggests that they formed by mechanisms other than stream incision. Little evidence exists to suggest that alternate mechanisms such as sheetwash or piping are active, whereas debris flows that originate in the soil mantle are common erosional events in the area, and relict debris-flow scars are abundant, particularly in the zero-order basins. Zero-order basins commonly are referred to as hollows to reflect the character of hillslope depressions.

A 6-km^2 area was examined to elucidate the relationship between debris flows and the development of hollows. The study area contains many debris-flow scars and a broad range in size and degree of development of hollows. Landslides and landforms were mapped in the three main drainages of the study area. This map information was then used to investigate the relationship between debris flows and hollows and to evaluate the likelihood that debris flows have carved these features. It was determined that the hollows

occupy only 25 percent of the total drainage plan area, but include 74 percent of mapped debris-flow scars.

The likelihood that debris flows carved the hollows within the Holocene was evaluated by assessing the geomorphic impact of a single storm event in 1986, which triggered 11 debris flows, and by extrapolating the effects of this storm to the long-term geomorphic impact that debris flows can have on the landscape. The February 1986 storm had a calculated return interval of 11 years, and moved 97 m^3 of soil from the hillslopes. A rough, order-of-magnitude estimate of the time to carve the hollows from planar slopes was made based on the storm data and an estimated 45,000 m^3 volume of all hollows. A time period of approximately 5,000 years appears sufficient to carve the hollows by storms of equivalent magnitude.

A model was created to describe the initiation of hollow formation from debris-flow events. Hollows appear to develop from the clustering of additional debris flows around isolated debris-flow scars. Hollows continue to grow from the recurrence of debris flows within the concavity, transporting soil and weathered bedrock from the slope to the channel below. The continuation of this process leads to hillslope forms that may, in time, expand to alter the overall morphology of the drainage basins.

INTRODUCTION

Understanding the relationship of geomorphic form to process is a major goal of geomorphology. A key to geomorphic research is the study of processes that repeatedly produce similar forms. In this category are landslides and other mass movements that systematically influence the geomorphic development of many landscapes by determining the style of erosion and deposition of material from hillslopes. The study of hillslope processes can best be performed in a setting where complexity is at a minimum, thus allowing study of specific relationships.

A landscape with a uniform and distinct form near the town of Sunol (fig. 1) in the eastern portion of the San Francisco Bay region is the subject of this thesis. The entire terrain is within a relatively youthful, uplifted terrace located adjacent to the Calaveras fault (fig. 2). The features of interest are similar appearing, unchannelized, concave hillslope depressions formed on the steep sidewalls of small, incised first-order drainages. The drainages have remnants of older, planar slopes now being altered and removed by the processes that formed the concavities, and the shape of these concavities suggests that they are not the result of the same fluvial processes that formed the drainages.

Many debris-flow-type landslide scars and related features were observed in the study area (fig. 3). The majority of the scars observed appeared to be within the concavities rather than on other portions of the hillslopes.

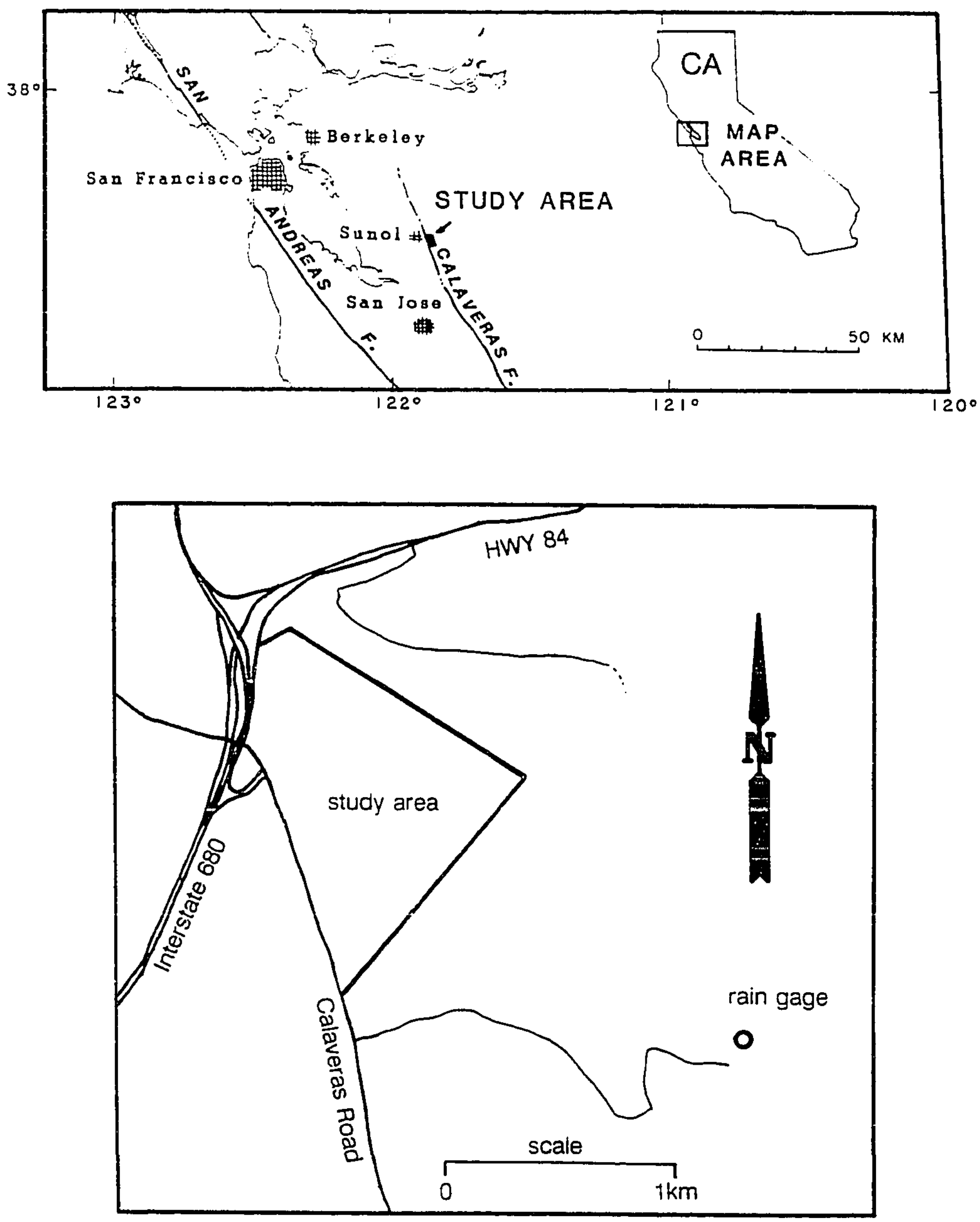

Figure 1. Location of study area.

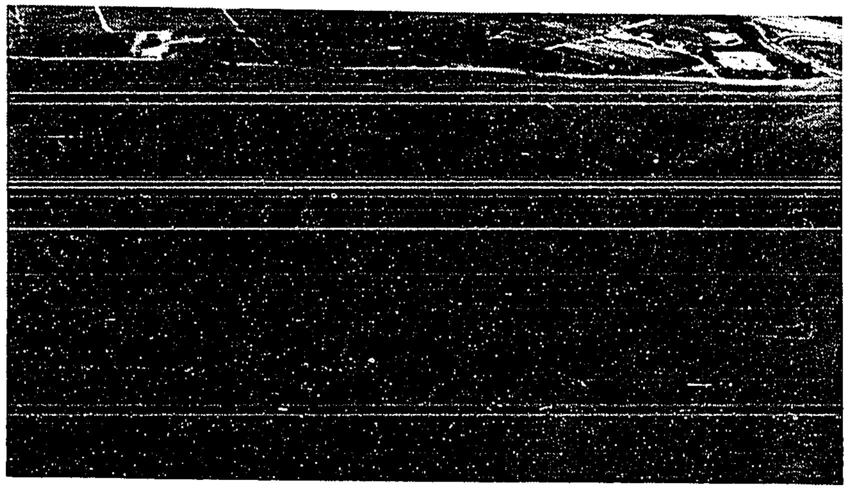

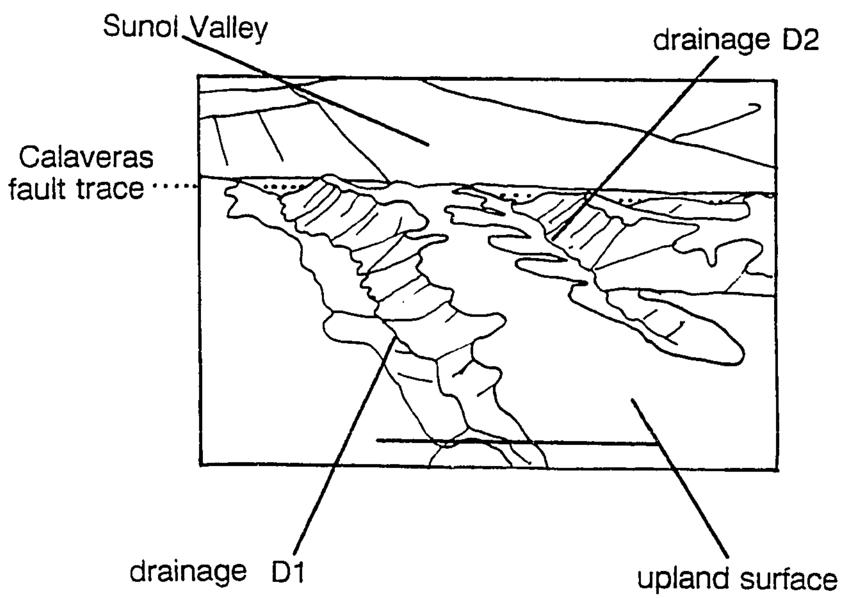

Figure 2. Aerial view of study area, looking west. Remnants of the uplifted terrace surface are visible between the valleys. The trace of the Calaveras fault trends from left to right near the top of the photograph.

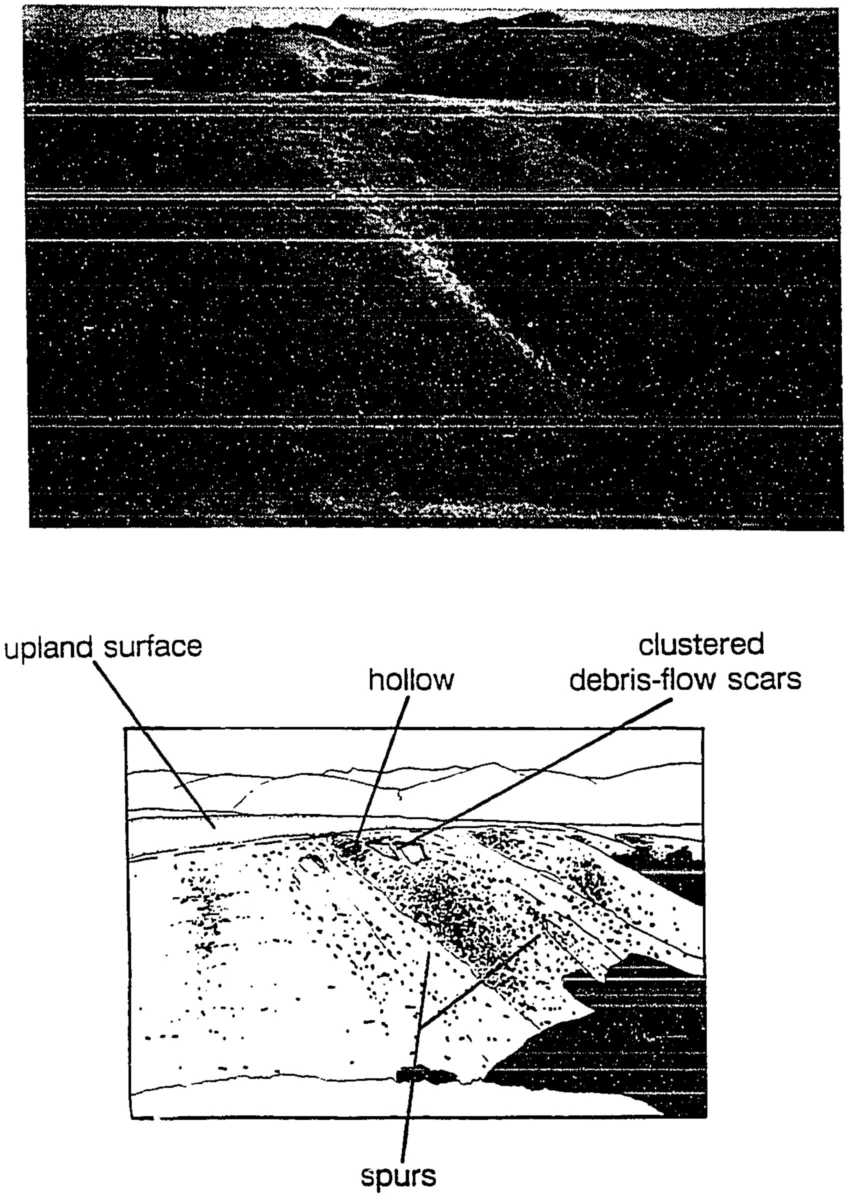

Figure 3. Debris-flow scars in upper portion of hollow.

Debris flows triggered during a rainstorm in 1986 provided an opportunity for observations of active processes.

The concavities function as zero-order basins as defined by Dietrich and others (1987). These types of hillslope features are recognized as an important part of the overall geomorphic system (Hack and Goodlett, 1960), because they are functional parts of the sediment routing within drainage basins. Zero-order basins commonly are called hollows, in part to separate them from the purely hydrologic implications associated with numbering legs of stream-drainage networks in the manner of Strahler (1964) and of unchanneled basins as used by Tsukamoto (1973).

Hollows also have become an important focus in landslide studies primarily because they have been identified as potential source areas for landslides. As such, their recognition in the field enhances the appraisal of specific landslide hazards. Hollows are defined by Hack and Goodlett (1960) and Hack (1965) as portions of hillslopes with contours concave-outward away from the ridge, contrasting with side slopes and noses where contours are straight and convex, respectively. Dietrich and others (1987) limit the definition of hollows to that of a purely topographic feature, the zone of concave contour lines, with nothing implied about genesis.

How do hollows develop? Little has been published specifically on the origin of these features. Events such as tree-root throw, single landslides, and gullying commonly have been cited as possible ways to initiate concave depressions (e.g., Reneau, 1988).

In the study area, hillslope processes have produced hollows showing a broad continuum of stages of development on hillslopes that are morphologically similar to each other. This similarity offered an opportunity to learn more about the development of hollows in a well constrained area. Although debris flows may not be responsible for the initiation and development of all hollows, it appeared that debris flows could be intimately involved with the initiation and enlargement of hollows within the study area.

The purpose of this thesis is to investigate the relationship between distinctive topographic form and current hillslope processes in the study area. The thesis will: 1) describe the morphology of the hollows, the debris flows, and the overall hillslopes, 2) address the question of what process(es) are responsible for the formation of the hollows, and 3) evaluate the relationship between the hollows and debris flows.

PREVIOUS WORK

Debris Flows

The term debris flow as used in this thesis represents a complex hillslope process, where flowage of debris is only part of the process. In the San Francisco Bay area, debris flows typically originate as soil slips (Ellen, 1988), shallow slides in the soil mantle that leave scars on hillslopes. The soil mass that fails can, under certain conditions, mobilize into flowing debris and move downslope. Debris flows leave characteristic features on the slope (fig. 4), which when preserved can tell a story about the landslide event.

Most debris flows occur on steep slopes, greater than 15 to 20 degrees, and are the result of abundant water in a failing soil mass (Costa, 1984). The focusing of groundwater flow, and the subsequent increase in soil pore water pressures, during high-intensity storm events on slopes with topographic convergence has been observed indirectly by several workers (Pierson, 1980; Sidle, 1984, 1986; Wilson and Dietrich, 1987; Reid and others, 1988). This concentrated increase in pore pressure is considered responsible for the localized initiation of soil failures, which are subsequently mobilized into debris flows. Pierson (1980) and Sidle (1984, 1986) have described such groundwater response to storm events in Oregon and Alaska, respectively. Reid and others (1988) and Wilson and Dietrich (1987) have recorded the development of

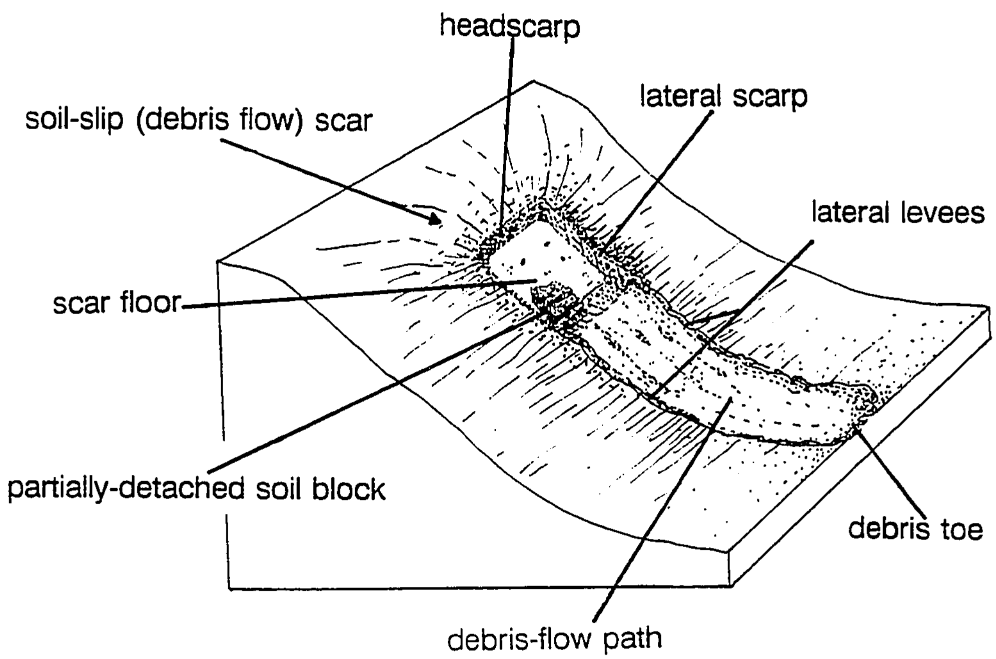

Figure 4. Typical features of a soil slip-debris flow.

positive pore pressures in areas of topographic convergence and bedrock focusing of groundwater flow during peak storm events in coastal California.

The soil initially fails in shear driven by gravity. The ability for this failure to become fluid, or to move as a debris flow, is dependent on site conditions and the physical characteristics of the soil (Ellen and Fleming, 1987). Costa (1984) has described the different styles of debris flows that commonly are observed, and he has shown how the variations of flow morphology can be ascribed to the range of grain size and clay content, water content, and inclination of slope.

Debris flow can be a rapid mass movement that is capable of substantial erosive power. This capability often enables debris flows to scour and alter land surfaces on which they travel. Debris flows also can pass over the landscape with minimal scour, leaving only trace deposits to mark their passage (Johnson, 1970). Because debris flows typically contain sediment concentrations greater than 80 percent by weight (Beverage and Culbertson, 1964), they are capable of efficiently transporting large volumes of material over the landscape.

Hollows

Small, unchannelized valleys are recognized as dominant features within the drainage areas of most soil-mantled hillslopes (Hack and Goodlett, 1960;

Dietrich and others, 1986). The valleys typically are present within the drainage basins upslope of low-order channels. The term zero-order basin (ZOB) has been used to describe the position of such valleys in the overall drainage system, because of their ability to influence the routing of sediment and runoff from source areas to the channels below (Dietrich and others, 1986). ZOBs are generally referred to as hollows, following the terminology introduced by Hack and Goodlett (1960) and Hack (1965) for the topographic shape represented by concave-out contours.

Hollows have gained importance in geomorphic studies because of the recognition that landslides commonly occur in their topographically convergent zones (Dietrich and others, 1986; Reneau, 1988). Many hollows develop thick mantles of colluvium (e.g., Hack and Goodlett, 1960; Pierson, 1977; Reneau, 1988). The hollows undergo infrequent, partial to complete evacuation of colluvium, usually when debris flows occur (Hack and Goodlett, 1960; Reneau and others, 1984; Dietrich and others, 1986; Reneau and Dietrich, 1987; Reneau, 1988). The focus of research on hollows has centered, in part, on their accumulation, storage, and periodic discharge of colluvial material (e.g., Dietrich and others, 1987). Although the process of accumulation of colluvium in hollows is recognized in many geomorphic settings, it is not necessarily the dominant process in all cases. Hollows can function simply as sediment routing features, developing and enlarging without the accumulation of material.

METHODS

Detailed field mapping of hillslope forms and distribution of debris flows in the study area was performed during the summer and fall of 1985. Subsequent visits were made during winter storm periods and at other times through the fall of 1988. An eight-time enlargement (1:3,000) of the U.S. Geological Survey 1:24,000-scale La Costa Valley 7.5-minute quadrangle was used as a base map for field observations of geomorphic features. Final map compilation was at a scale of 1:3,000. Symbols were selected to locate the various geomorphic features observed in the field on the base map, such as debris-flow scars, hollows, spurs, channels, gullies, and surfaces.

During mapping, it became evident that both fluvial and debris-flow deposits were present in the narrow valley bottoms (fig. 5). Although these deposits suggested interesting hillslope-channel interactions, the decision was made not to study the channel deposits, but to limit the scope of study to the role of debris flows in hillslope evolution.

During the summer of 1985, an inventory of the distribution of historical landslides was prepared from both field observations and aerial photos, and the landslides were located on the base map with symbols. This inventory was updated after each subsequent storm up to 1987. Fresh debris-flow deposits and scars were then studied to better understand their mechanics.

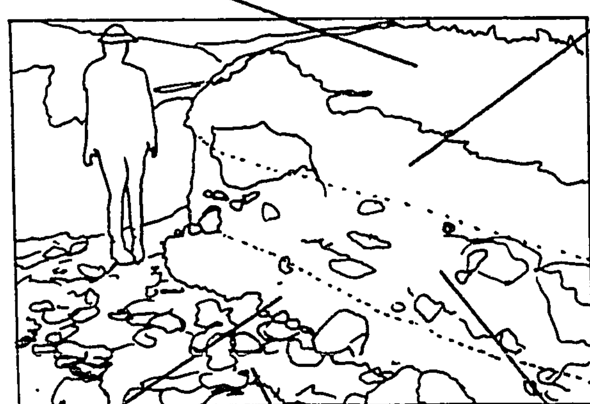

Figure 5. Exposure of deposits from several debris flows. Debris-flow deposits appear as matrix-supported cobbles. Finer-grained material interbedded with cobble lenses suggests that soil-dominated debris flows also occurred. Debris-flow deposits appear to overlie cross-bedded fluvial deposits at the base of the exposure. Bed of the active channel is to the left of the exposure.

Fresh scars, as well as old scars, were examined and analyzed for the progression of scar weathering and regression, and for the long-term process of soil regeneration. Soil samples collected from debris-flow deposits, scars, and undisturbed headscarps were tested for Atterberg limits and grain-size gradation by the U.S. Geological Survey Engineering Laboratory.

In an attempt to describe the form of hollows and to model their morphogenesis, various field studies were performed to define their shape relative to the surrounding landscape. Profiles were measured down the axes of four hollows that represented the range in volume from the largest to one of the smaller in the area. The profiles were constructed by measuring the slope inclination at 1-m intervals from the crest to the base of the slope. Slope inclinations also were measured around portions of the perimeter of two drainages to develop data on the ranges of slope steepness associated with different geomorphic slope features. These measurements were made with a hand-held Sunto clinometer from points on the upper edges of the drainages that allowed consistent sightings down each slope section.

Soil thickness and character were logged within one typical hollow. Eight pits were dug to bedrock; two on a surface upslope from the hollow, four in the hollow, and two on adjacent spurs. Pedologic descriptions were prepared for each profile. In addition, soil thickness was estimated in several locations based on profiles exposed in landslide scars.

Calculations of slope area and drainage volume were made with a planimeter by tracing contour lines in each of the three main drainages. Order-of-magnitude estimates of erosion rates were made by comparing the volumes of hollows to those of debris-flow scars.

SETTING

Location

The study area is located in the eastern San Francisco Bay region on land owned by the San Francisco Water Department and it is in the watershed for San Antonio Reservoir, east of the town of Sunol. The western and northern edges are bounded by Calaveras Boulevard and Highway 84, respectively (fig. 1). The remaining boundaries are drawn uphill of the area of study.

Landforms

The study area consists of an upland terrace surface dissected by three main drainages and four minor ones (fig. 6) that are all in a youthful stage of development (hypsometric disequilibrium of Strahler, 1964). The terrace surface is a broad upland of gently rolling hills. Plate 1 (in pocket) shows the observed locations and shapes of selected geomorphic features in the study area. Figure 7 shows the same feature locations at a smaller scale. The degree of development of all the drainages strongly suggests that they have formed after the terrace surface was first uplifted.

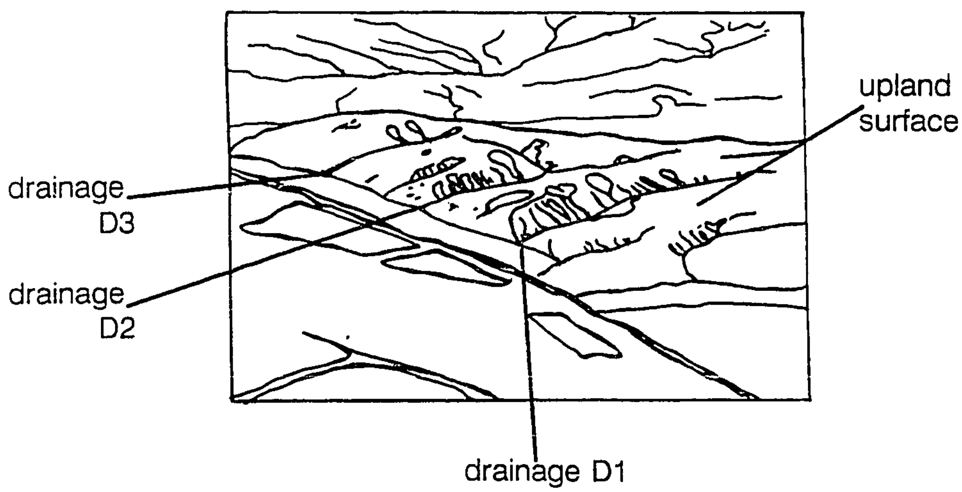

Figure 6. Aerial view looking to the northeast, with the study area in the center of the photograph. The degree of incision of the streams into the uplifted terrace is evident. The three main drainages are noted.

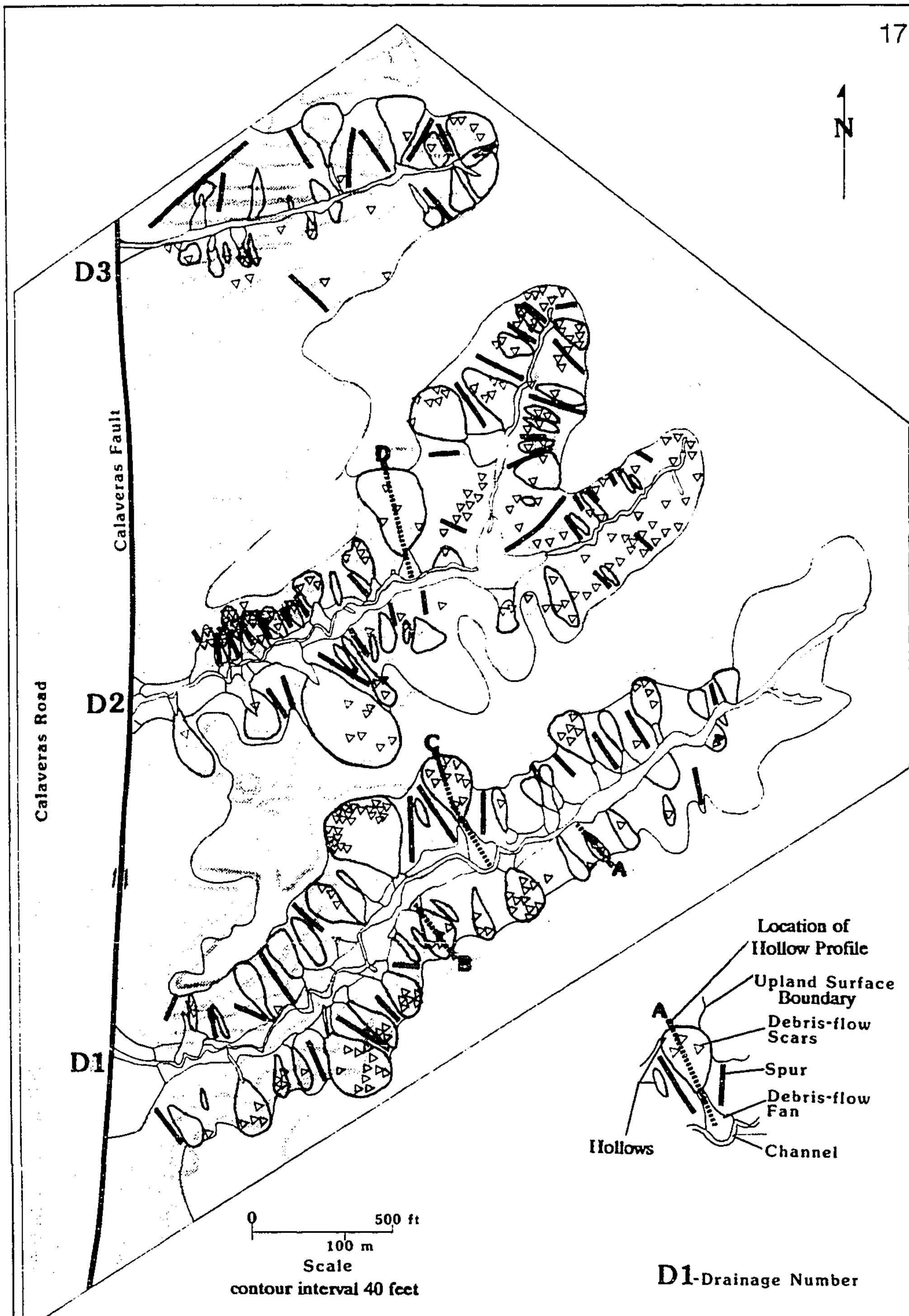

Figure 7. Location map showing selected geomorphic features in the study area.

Drainages

The southernmost valley in the study area, labeled D1 on figure 7, has the greatest relief (70 m) and drainage area (9,000 m^2). A narrow, stepped gully (fig. 8) in the oroad swale at the valley head widens down valley to a well defined, sinuous channel that is 0.5 to 6.0 m wide and less than 2.0 m deep. The two incised valleys to the north (D2 and D3), shown in figure 7, are shorter and end abruptly at steep headwalls (fig. 9). These two drainages have more poorly developed channels in their axes, and these are clogged with colluvial deposits (fig. 10). All streams in the area are ephemeral, flowing primarily during and immediately after storm events.

Hillslopes

Valley slopes are similar in appearance in all three drainages (fig. 2). When viewed along stream axes, the slopes appear as roughly planar surfaces dissected by concave depressions of varied size. These depressions are grossly bowl-shaped in overall form and are here referred to as hollows. Between many hollows are small spur ridges, here called spurs, that are often eroded remnants of the planar valley sideslopes. The hollows appear to be younger than the drainages and their remnant planar slopes. The hollows are eroding back into the older surfaces and ultimately may remove all evidence of the old slopes.

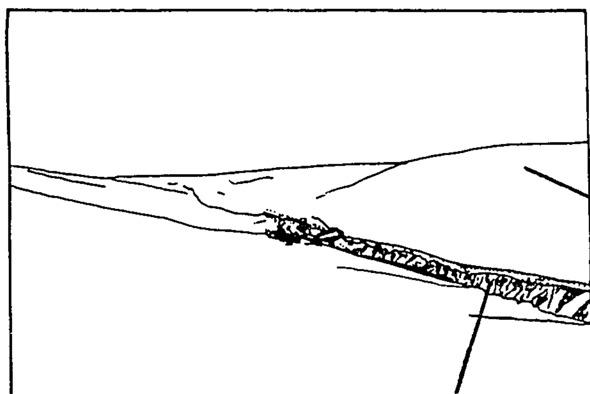

Figure 8. View to the east in the upstream part of drainage D1, showing headward portion of the spill-pool-floored gully. The gully has eroded down through a mature, argillic soil formed on old colluvium, and has reached the colluvial contact with bedrock near the right edge of figure.

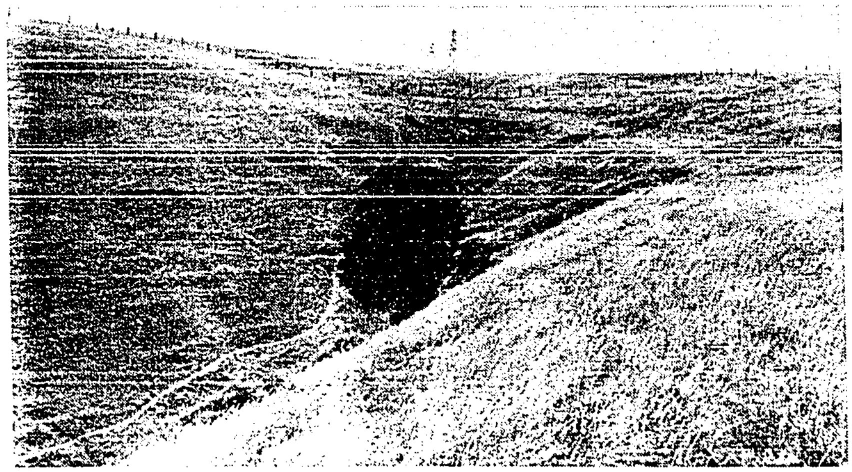

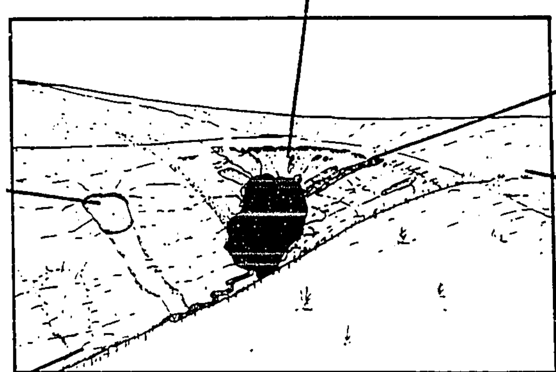

Figure 9. View of stream head of drainage D2 with abrupt headwall, showing extensive slumping (center) and discrete debris flows (left) on the slopes. Drainage area upslope from channel head is underlain by older colluvium.

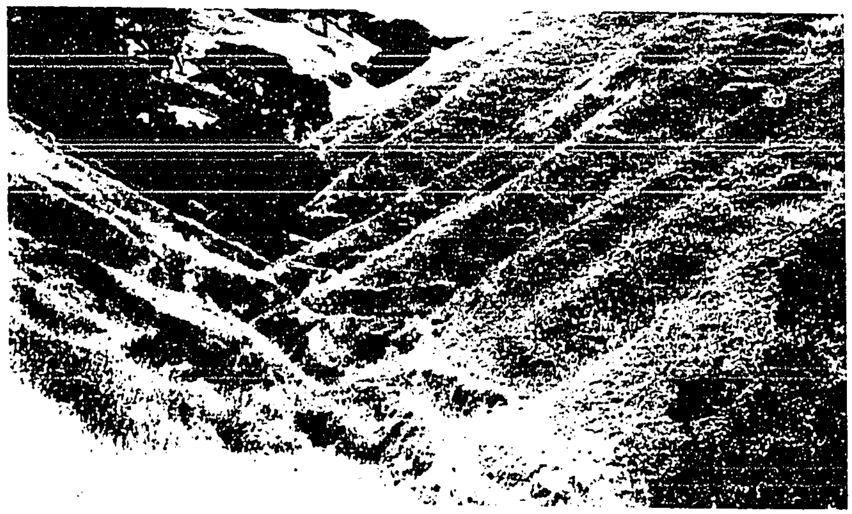

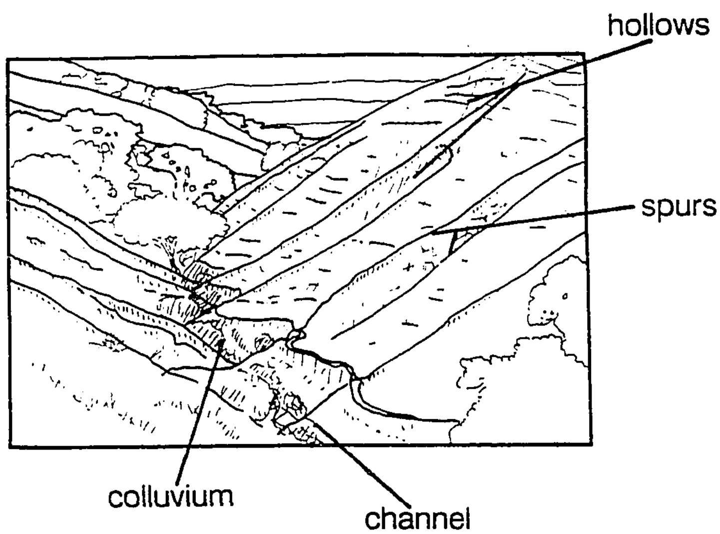

Figure 10. View downstream in drainage D3. Stream channel is discontinuous because the ephemeral stream is not removing all of the colluvial material in the channel.

Planar Slopes. The overall valley morphology and drainage pattern are roughly preserved in all three drainages in the form of the relict slope segments (fig. 6). The drainages are basically linear, with planar slopes (fig. 11). The subparallel, planar appearance of the pre-hollow valley walls (fig. 12) is still evident in every drainage in the study area. If the hollows did not exist, the entire drainages would likely have consistent slopes. The planar slopes appear to predate the development of the hollows.

Spurs. The spurs are relict portions of the earlier valley sideslopes and are formed where two hollows are adjacent on the slope (fig. 13). They appear as narrow ridge segments oriented perpendicular to the main channel. The alignment of the spurs is most obvious when looking downstream, and the plane formed by the spurs can be used to trace the form of the pre-hollow slopes (fig. 14).

Hollows. The most noticeable topographic features in the study area are the hollows (fig. 15). They function as zero-order source areas for the first-order stream that flows down the axis of each drainage. The hollows in the study area are unchannelized concavities that are all similar in axial profile and geometry. They appear egg-shaped in plan view (fig. 7) and typically are funnel-shaped when viewed straight on (fig. 16).

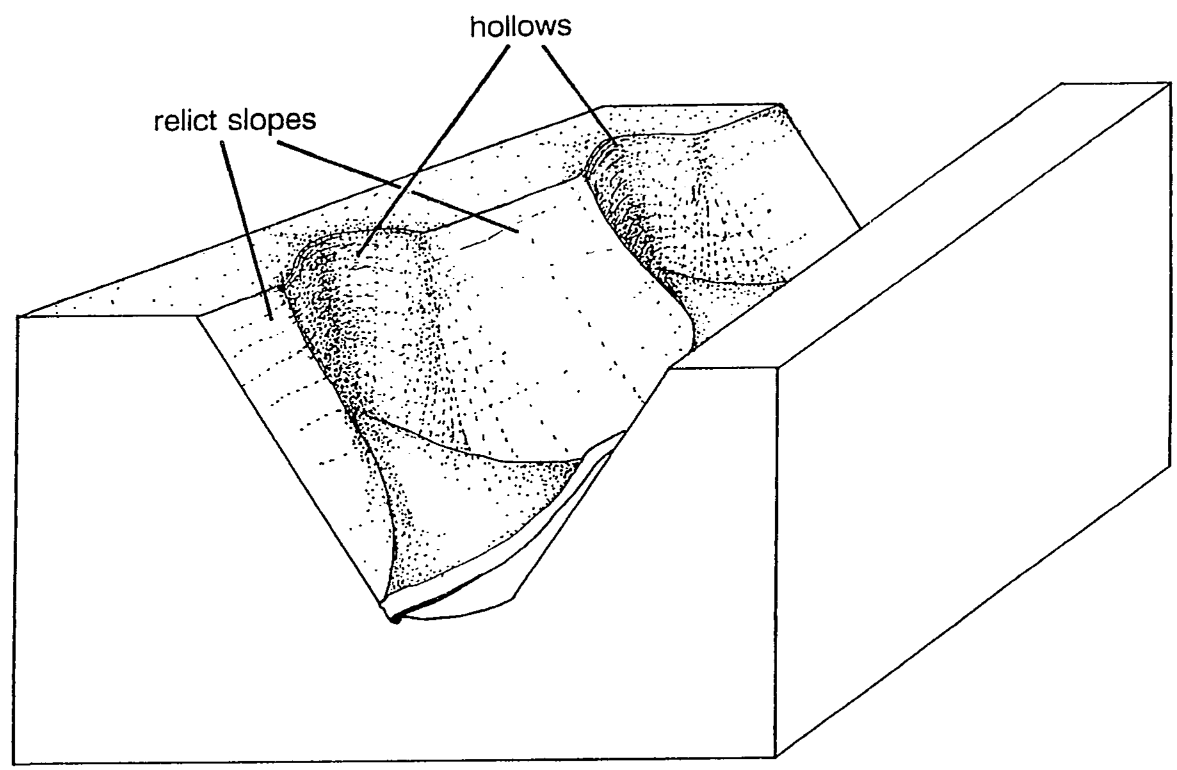

Figure 11. Diagram of typical linear drainage with planar slopes dissected by hollows.

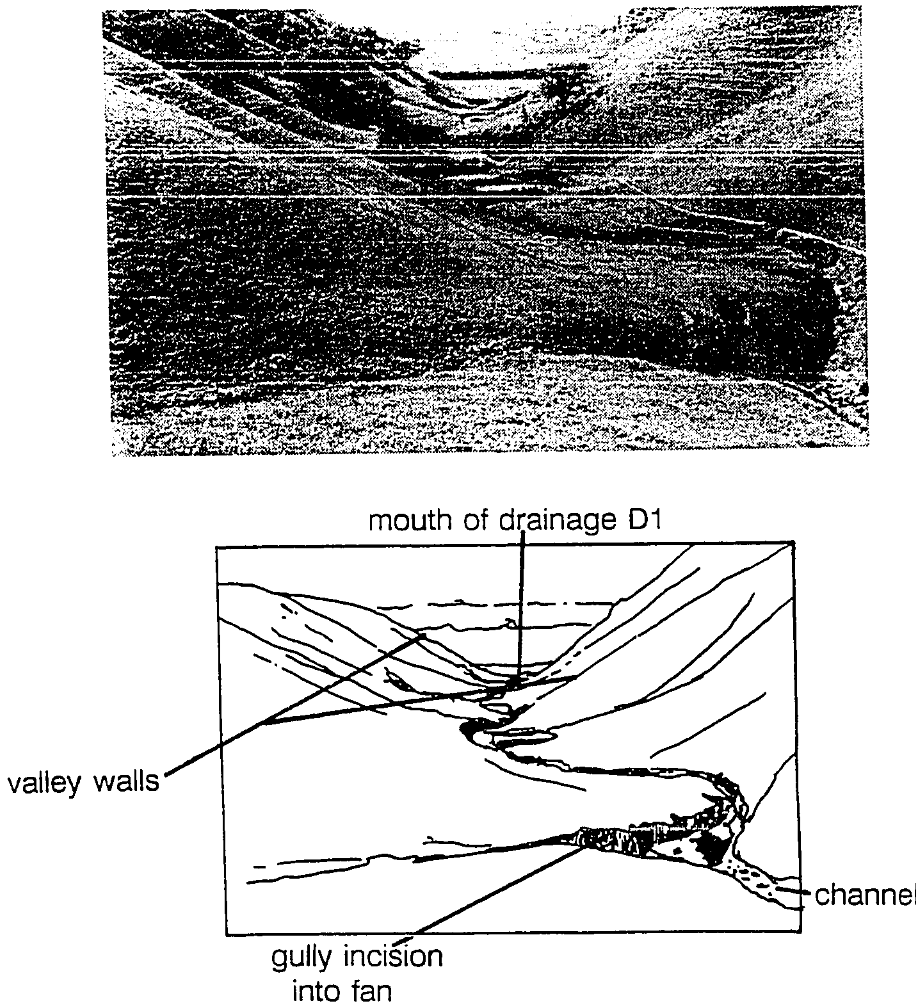

Figure 12. View downstream in drainage D1. The subparallel, planar appearance of the pre-hollow valley walls is evident. Meandering of the intermittent stream is amplified by encroachment of small colluvial fans from the mouth of each hollow.

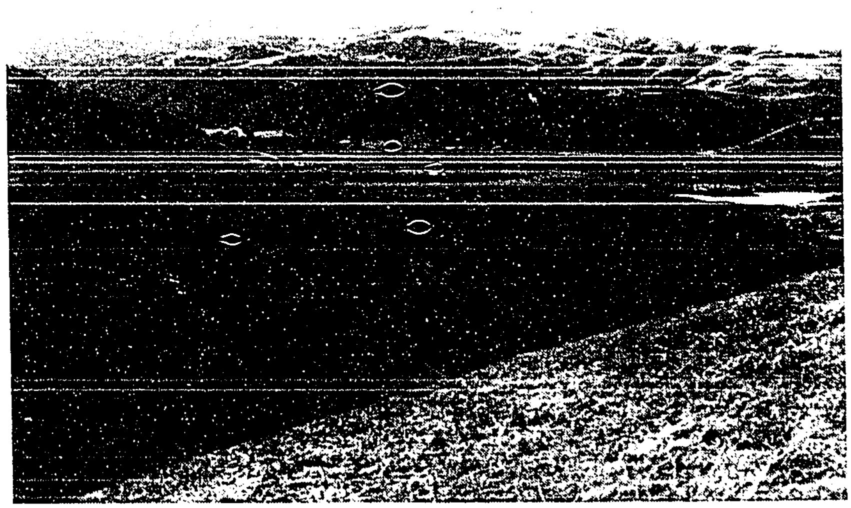

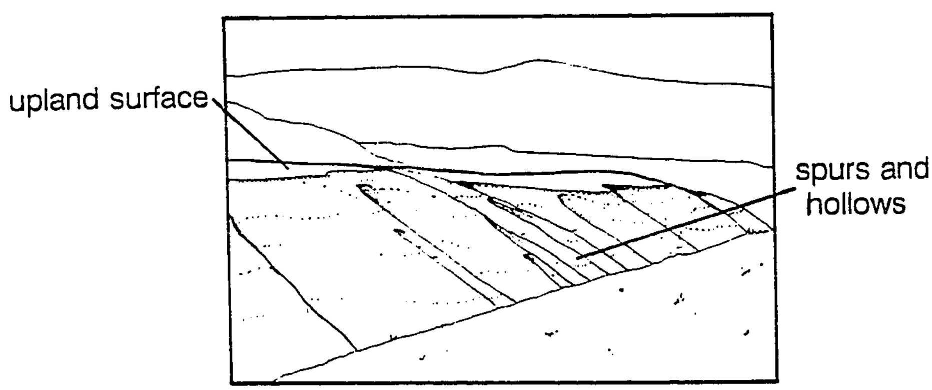

Figure 13. View southward across drainage D1, showing the active slopes of the incising drainage in contrast to the stable upland surface. Spurs appear as linear ridges between hollows.

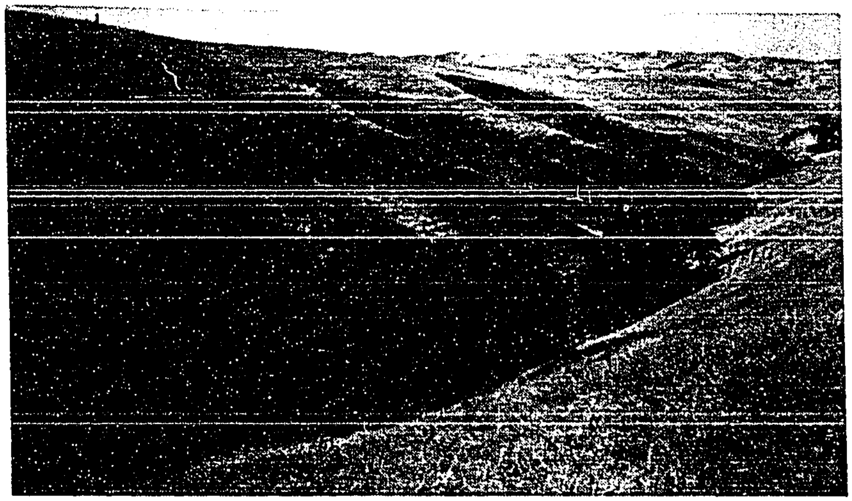

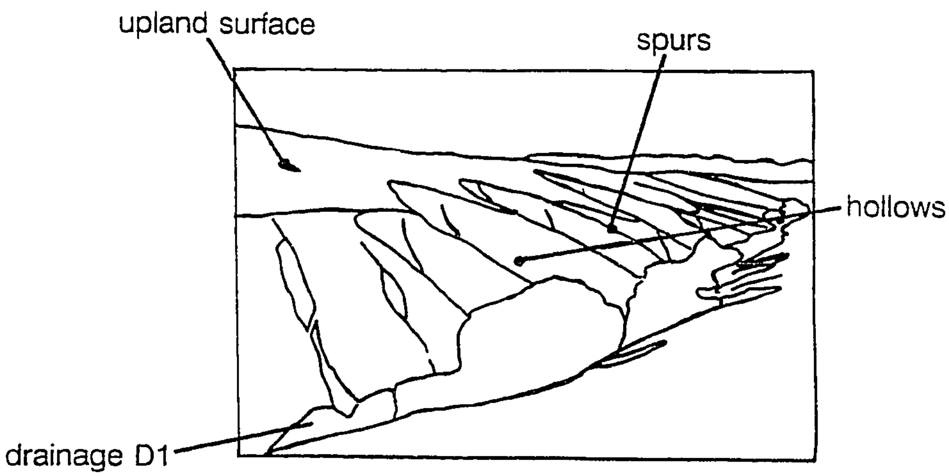

Figure 14. View northeast of the gently sloping upland surface and the sidewalls of drainage D1. The spur ridges between the hollows are formed from the old planar slopes of the drainage.

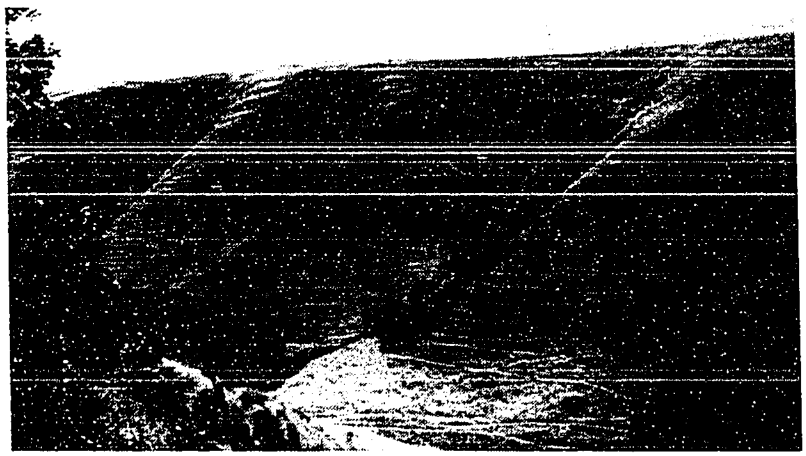

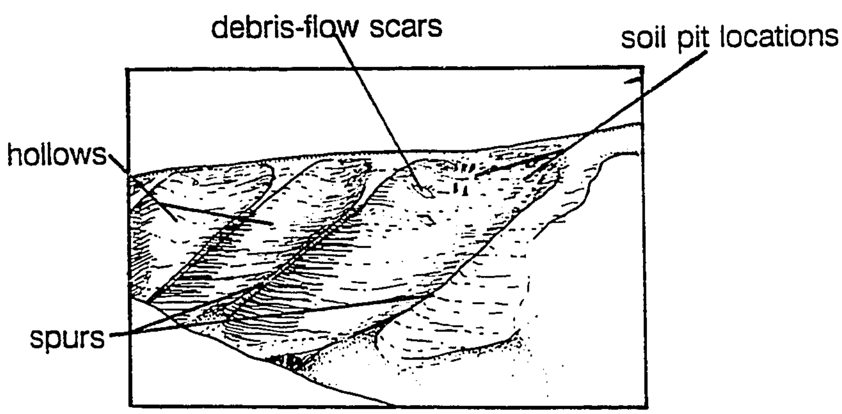

Figure 15. View of north-facing slope of drainage D1, which exhibits well developed hollows and spurs. Hollows appear as concave depressions on the hillslope. The location of soil pits dug in one hollow is noted, as discussed in text.

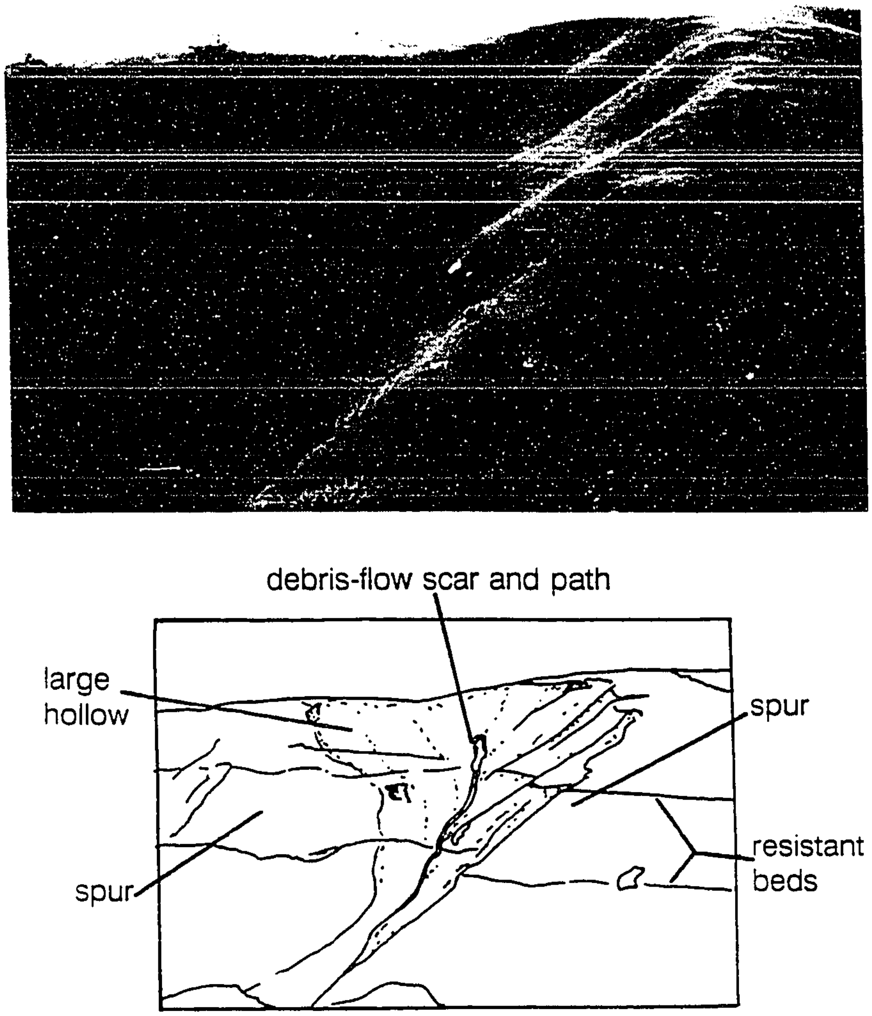

Figure 16. The largest hollow in the study area, showing the typical funnel-shaped form. Funnel shape can be seen by tracing the margins of adjacent spur ridges down towards the channel. Note the single debris-flow scar and flow path which occurred during the February 1986 storm. Debris traveled all the way down to the main drainage. Two outcrops of resistant conglomerate beds of the Livermore Gravels are exposed on the hillslope.

Stratigraphy

Bedrock

The Pliocene-Pleistocene, upper Livermore Gravels, which constitute bedrock in the study area, rest unconformably on upper Tertiary continental and marine rocks both in the immediate study area and over much of the southern Livermore Basin. The Tertiary rocks in turn overlie rocks of the upper Mesozoic Franciscan Complex and Great Valley Group (Dibblee, 1980; Barlock, 1989; Isaacson, 1990).

The Livermore Gravels (Clark, 1930) consist of moderately to poorly lithified pebble and cobble conglomerate of terrigenous origin (fig. 17). Clasts commonly are of Jurassic to Cretaceous Franciscan Complex rocks, derived from a Diablo Range source area to the southeast (Barlock, 1989). Red chert, vein quartz, schist, and graywacke cobbles are common throughout the area, and rounded mudstone clasts are rare.

One to three resistant beds, 2 to 6 m thick, commonly are exposed in the side walls of each valley of the study area (fig. 15). These beds are coarser grained and appear to have relatively better cementation than adjacent beds to account for their erosional resistance.

The upper Livermore Gravels are interpreted to be of Pliocene and/or Pleistocene age in this area (Ollenburger, 1986). Herd and Brabb (1980)

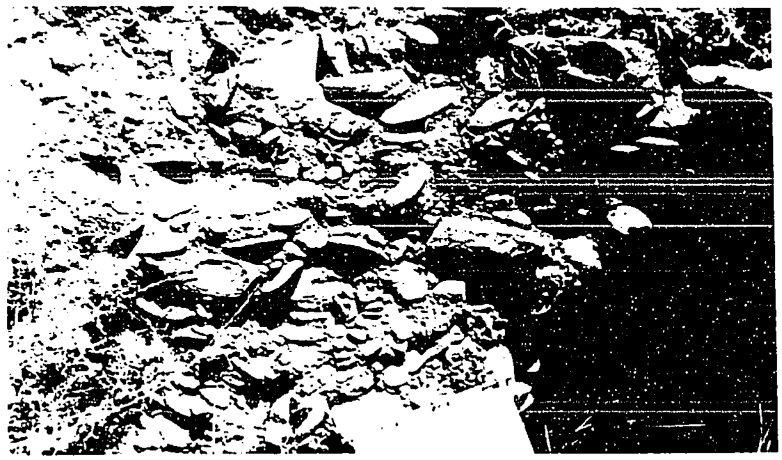

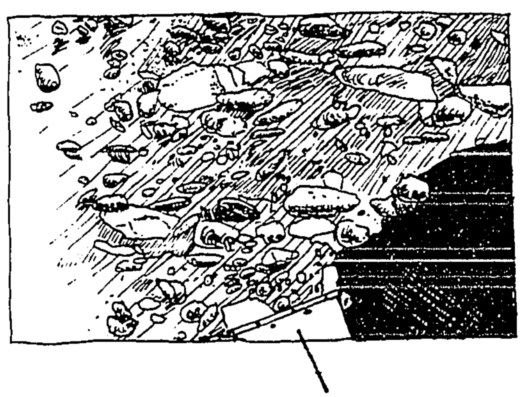

Figure 17. Close-up view of an outcrop of cemented Livermore gravels. Rounded clasts exhibit slight imbrication. Matrix is clay rich with possible calcite cement. Clast size ranges from 1 to 10 cm. Field of view is approximately 1 m in height.

reviewed the paleontological data available for the Livermore Gravels and concluded that the uppermost part of the gravels, exposed as terrace surfaces, is between 300,000 and 600,000 years old. These particular terrace surfaces are northeast of the study area and probably are similar in age to the upland surface of the study area.

Colluvial Deposits

Broad zones of old colluvium are exposed at the heads of the main drainages and appear as slightly concave depressions in the upland surface, commonly near the edges of the drainages (fig. 18). The deposits have a plan view appearance that is similar to that of the larger hollows (plate 1); however, the field appearance of the deposits is much more subdued than the hollows. The spatial relationship between this old colluvium and the upland surface suggests that the colluvium is closer in age to the upland surface of Herd and Brabb (1980), and predates the present setting under which the hollows have formed.

The colluvium consists of a fine-grained matrix with scattered small, gravel-sized clasts (fig. 19). The soil developed on the colluvium is redder than the soils described below, which, combined with the finer-grained texture, suggests that the colluvium is the result of low-rate depositional processes.

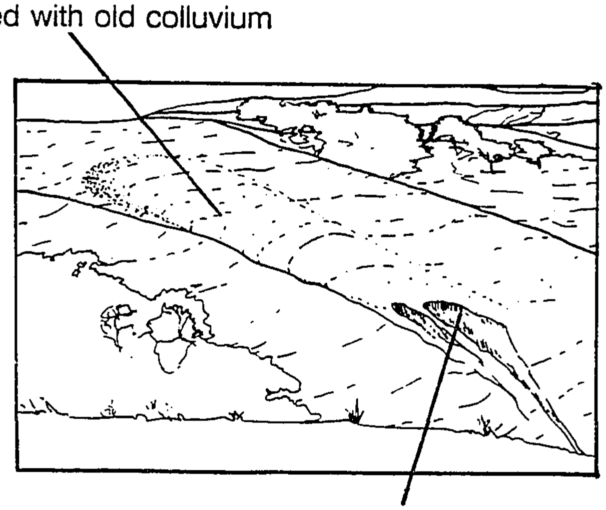

Figure 18. Deposit of old colluvium. Debris flows have only partially mobilized in the immature soils immediately downslope from the lower termination of the colluvium.

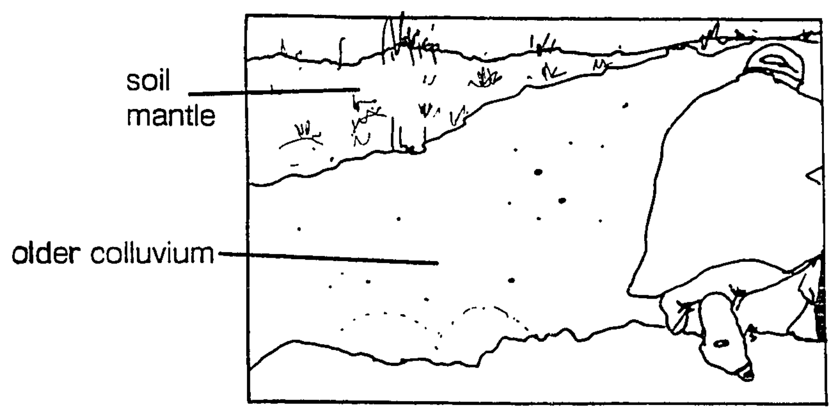

Figure 19. Exposure of old colluvium at the head of Drainage D2. The colluvium is fine grained, with scattered pebbles in a clayey matrix that has reddish coloration as well as clay coatings and bridging between grains.

Soils

Two major soil types are present in the area. Both have been mapped by the Soil Conservation Service (SCS) as Positas gravelly loam, subclassified as either 2 to 20 percent slopes, or 40 to 60 percent slopes (Welch and others, 1966). The upland surface has a mature soil profile up to 4 m thick overlying bedrock; this represents the SCS subunit of 2 to 20 percent slope. Less developed soils that exhibit little horizonation occupy the steep hillsides along the drainages. These represent the SCS subunit of 40 to 60 percent slopes.

Detailed soil-profile descriptions are contained in Appendix I. Both soil types commonly contain a high percentage of clasts (50 to 80%). In a typical soil profile, the friable mudstone clasts appear to be the first to weather, followed by the graywacke. By comparison, the siliceous rocks, cryptocrystalline vein quartz and red chert, appear to be only slightly weathered and are present throughout the profile. Vein-quartz pebbles and cobbles commonly are visible on top of the older terrace surface. All clasts are well rounded, reflecting the alluvial origin of the bedrock.

Soil thickness, measured vertically, was observed to be approximately 1 m throughout most of the hollows, as well as on the slopes between hollows. Soils mantling the upland surface are on the order of 2 to 4 m thick.

Structural Geology and Tectonics

The western edge of the study area follows the Calaveras fault (fig. 20), which is an active, right-lateral, predominantly strike-slip fault, a major tectonic feature of central California (Burford and Sharp, 1982). Offset began along the 130-km-long fault as early as 3.6 Ma, and the fault has a total slip of 16 to 24 km (Page, 1982). A minor vertical component of movement has uplifted ground on the east side of the fault in this area and formed an escarpment as much as 55 m high (fig. 21).

Bedrock in the Sunol Valley region is deformed into a series of folds. Adjacent to the study area, Tertiary and Cretaceous bedrock is cut by a number of reverse faults (Dibblee, 1980). The Livermore Gravels are essentially undeformed in this area and display more-or-less uniform structural dips of less than 10 degrees to the northeast.

Climate

The region has a Mediterranean (xeric) climate. Rainfall averages 50 to 54 cm/yr (Rantz, 1971) and falls primarily during the winter months. During the period of study, from 1984 to 1988, only one storm of a magnitude great

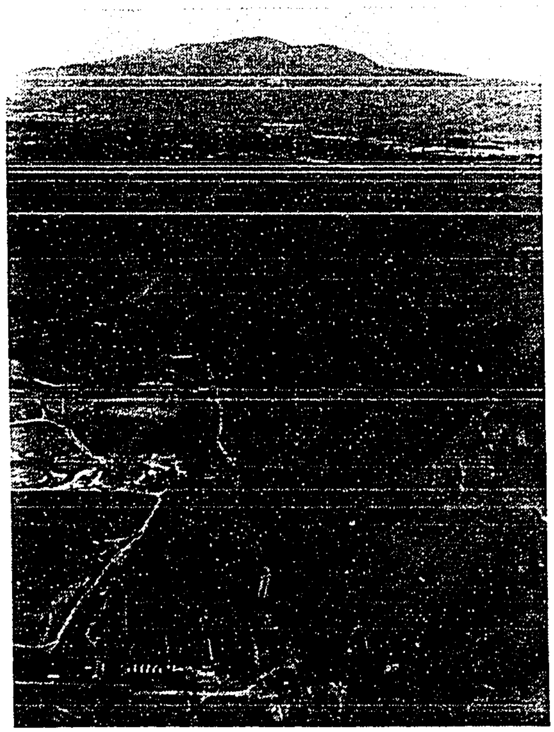

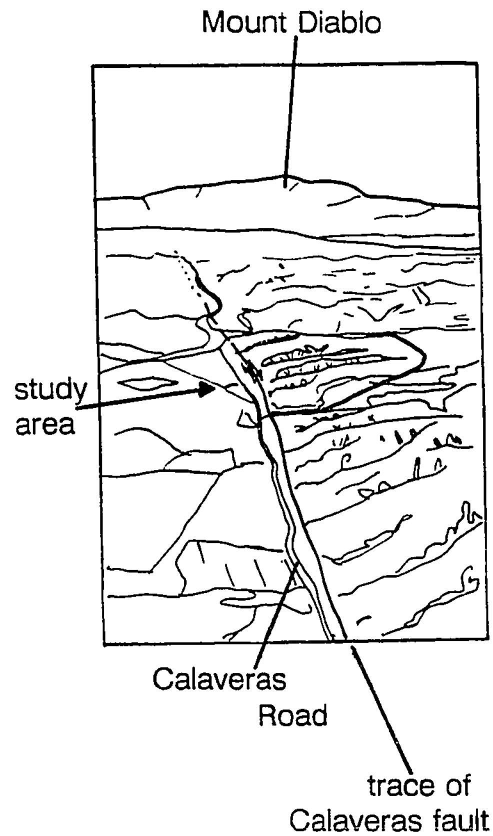

Figure 20. Aerial oblique view looking north up the Sunol Valley. Uplift in the area of study has occurred on the east side of the Calaveras fault (Page, 1982).

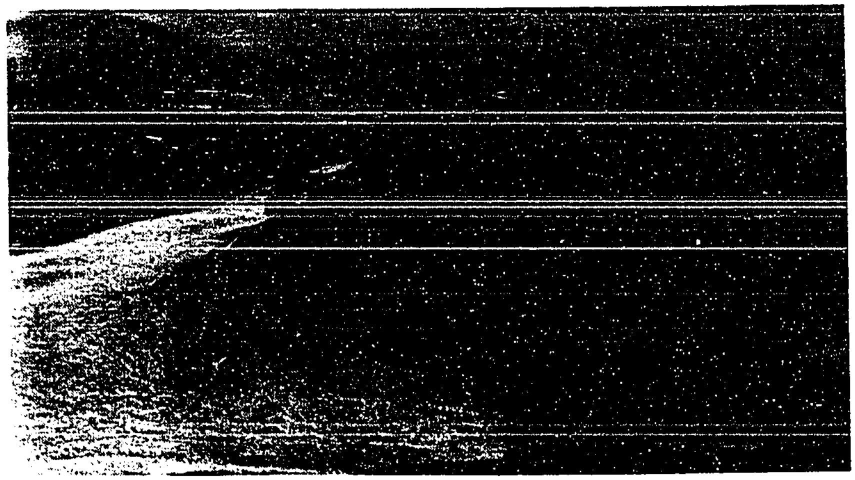

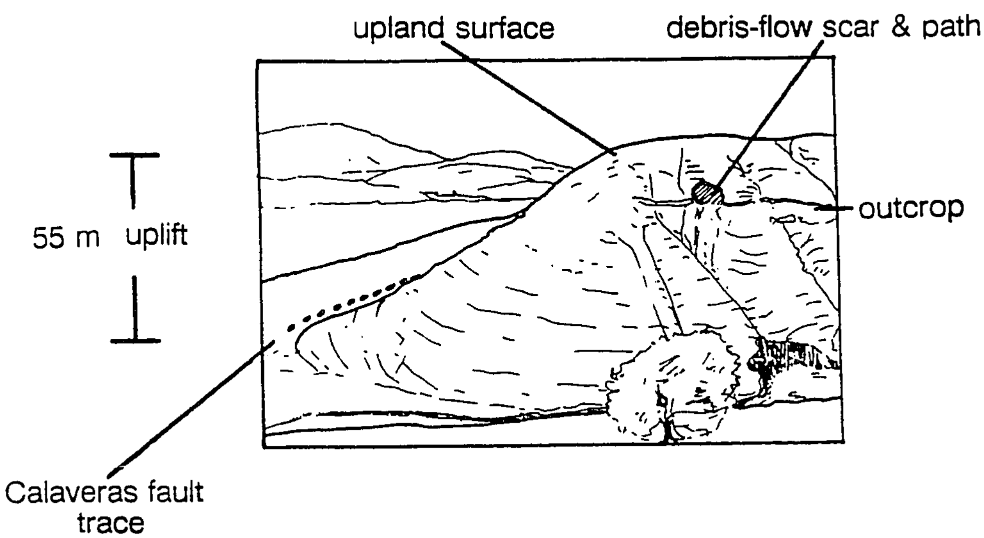

Figure 21. View north across the mouth of drainage D1, showing the uplift that has occurred along this portion of the Calaveras fault.

enough to trigger debris flows occurred. This storm of 12 to 21 February 1986 produced a total of 19.05 cm (7.5 in) of rainfall during the 10 day period.

Vegetation

Vegetative cover is annual grasses and forbs, with scattered trees of Valley Oak (*Quercus lobata*) and California Buckeye (*Aesculus californica*) clustered on the shaded sides of the valleys. Grazing by cattle has been common for over a century in this area. The impact of grazing has been to promote expansion of grass cover by consumption of small trees. In addition, unvegetated sidehill cattle paths have created terracettes that are present throughout the area (fig. 22).

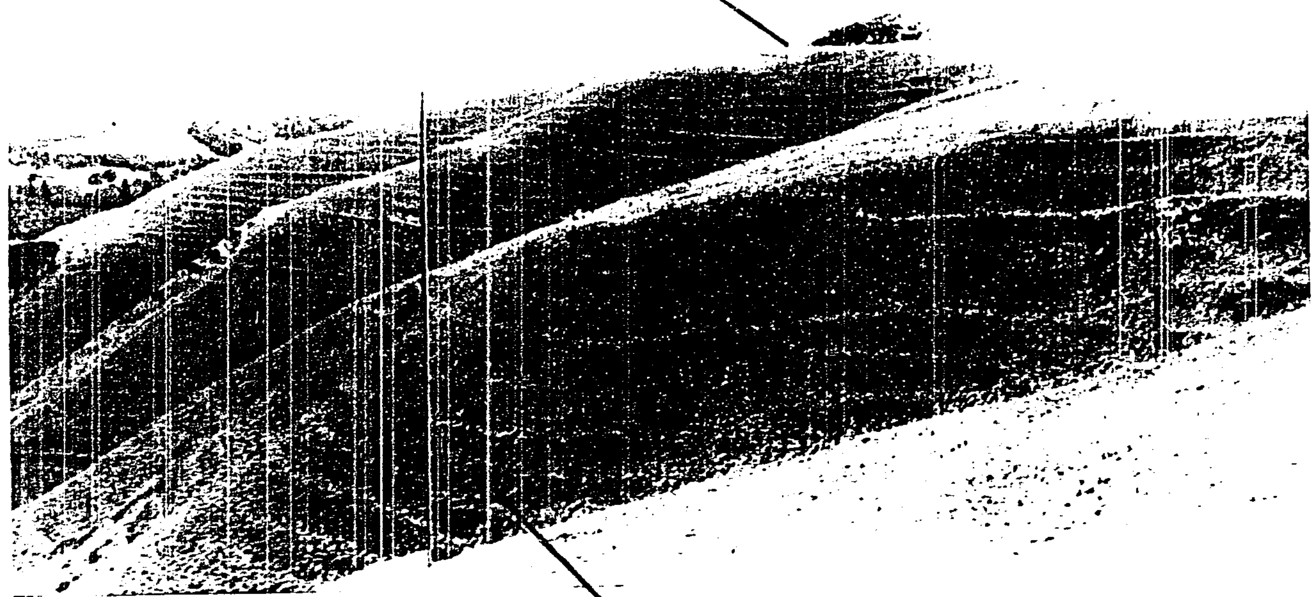

Figure 22. Terracettes are common on steep hillslopes along drainages throughout the study area.

HOLLOW MORPHOLOGY

The form, or morphology, of the hollows in the Sunol study area is consistent across the range of sizes observed. This section of the thesis describes the shapes of the hollows and includes a zonation of slope segments to assist in their analysis. Plate 1 shows the observed locations and shapes of selected geomorphic features in the study area. Every recognizable hollow in the three main drainages is included on plate 1, as well as the majority of the spurs and the location of all observed debris-flow scars. The plan-view shape of the hollows is best seen on plate 1. Terminology used in describing the hollows is presented in figure 23.

Physical Description

The hollows in the study area (plate 1) are estimated to range from 100 m^3 to 3,400 m^3 in volume. The smallest hollows are recognizable by having a slightly concave topographic form and an incised volume greater than one or two average debris-flow scars (fig. 24). Larger hollows stand out by their abrupt departure in form from the relict planar slopes (fig. 25). They typically have broad, gently-curved backslopes that merge with the sideslopes shared with adjacent spurs. The backslope narrows in the downslope direction, creating the visual impression that the spurs become closer together toward the

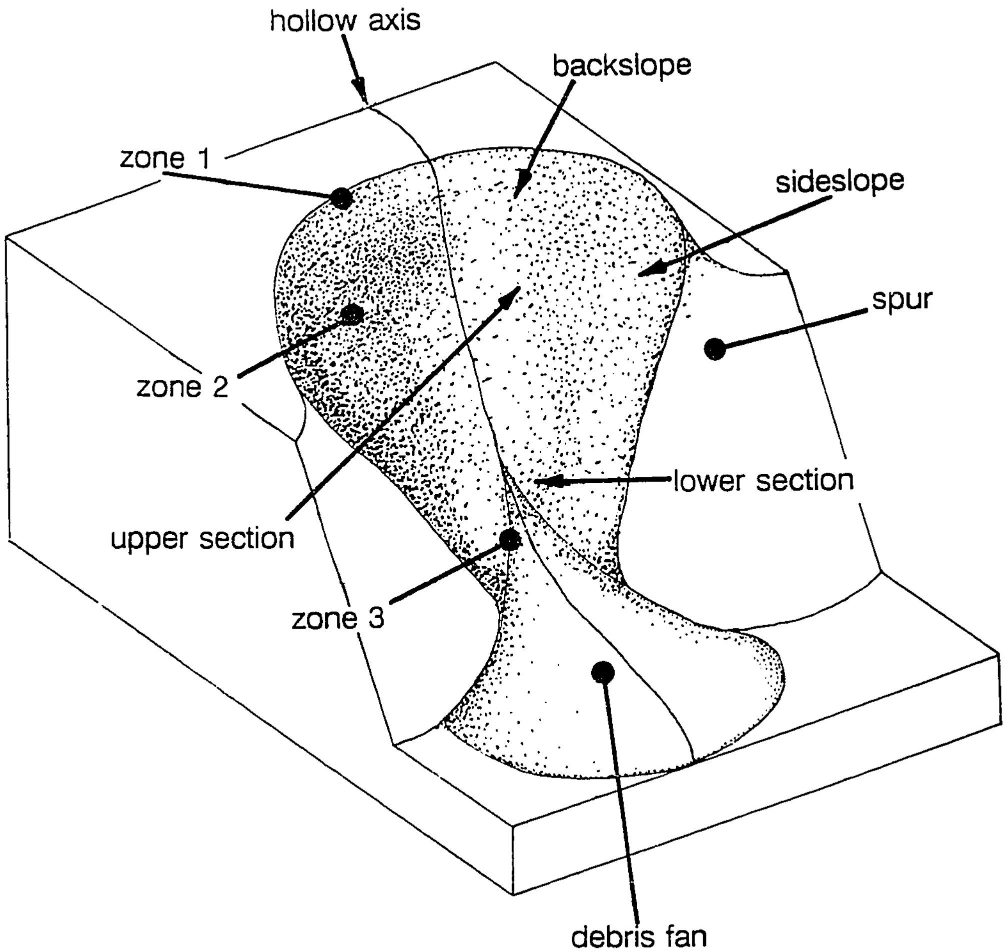

Figure 23. Diagram of typical hollow features, showing terminology used in text.

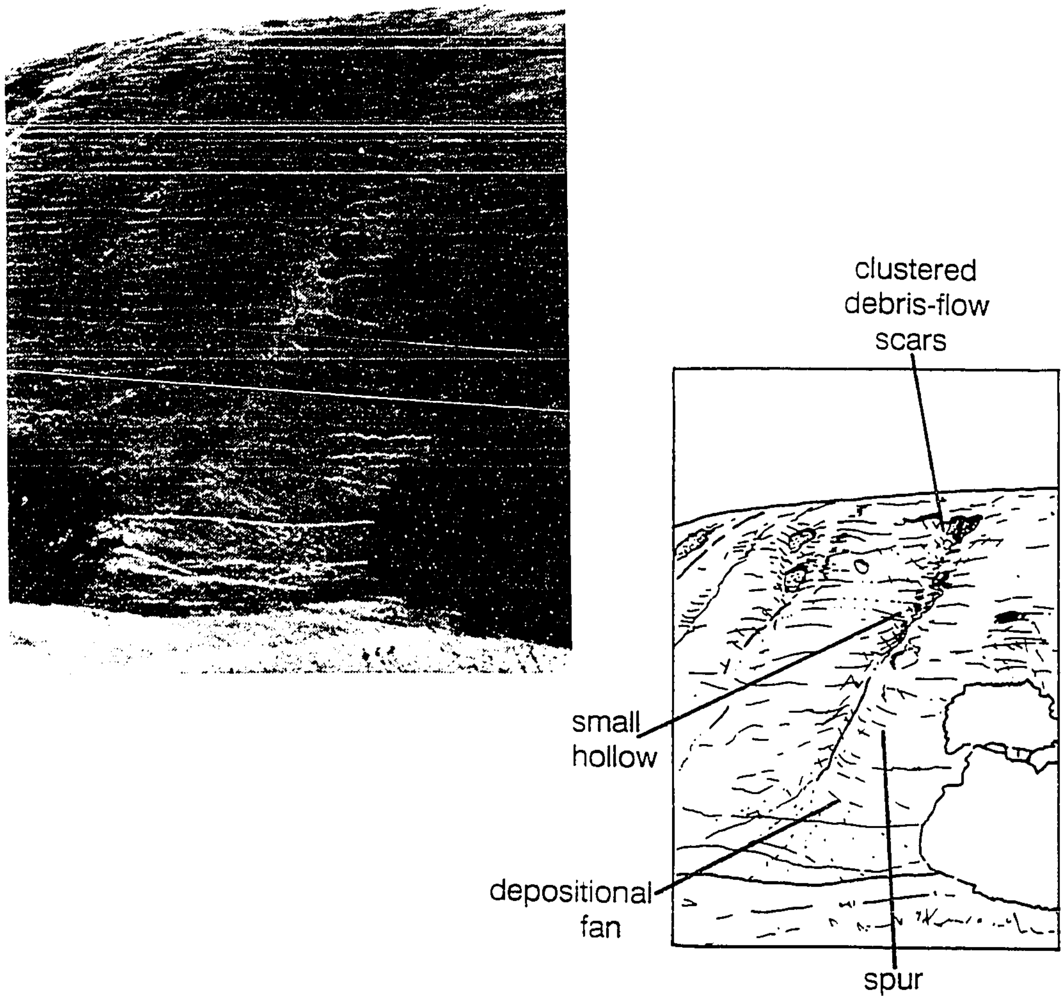

Figure 24. View of one of the smaller hollows in the study area. Hollow development has progressed enough to allow identification of key features of a typical hollow.

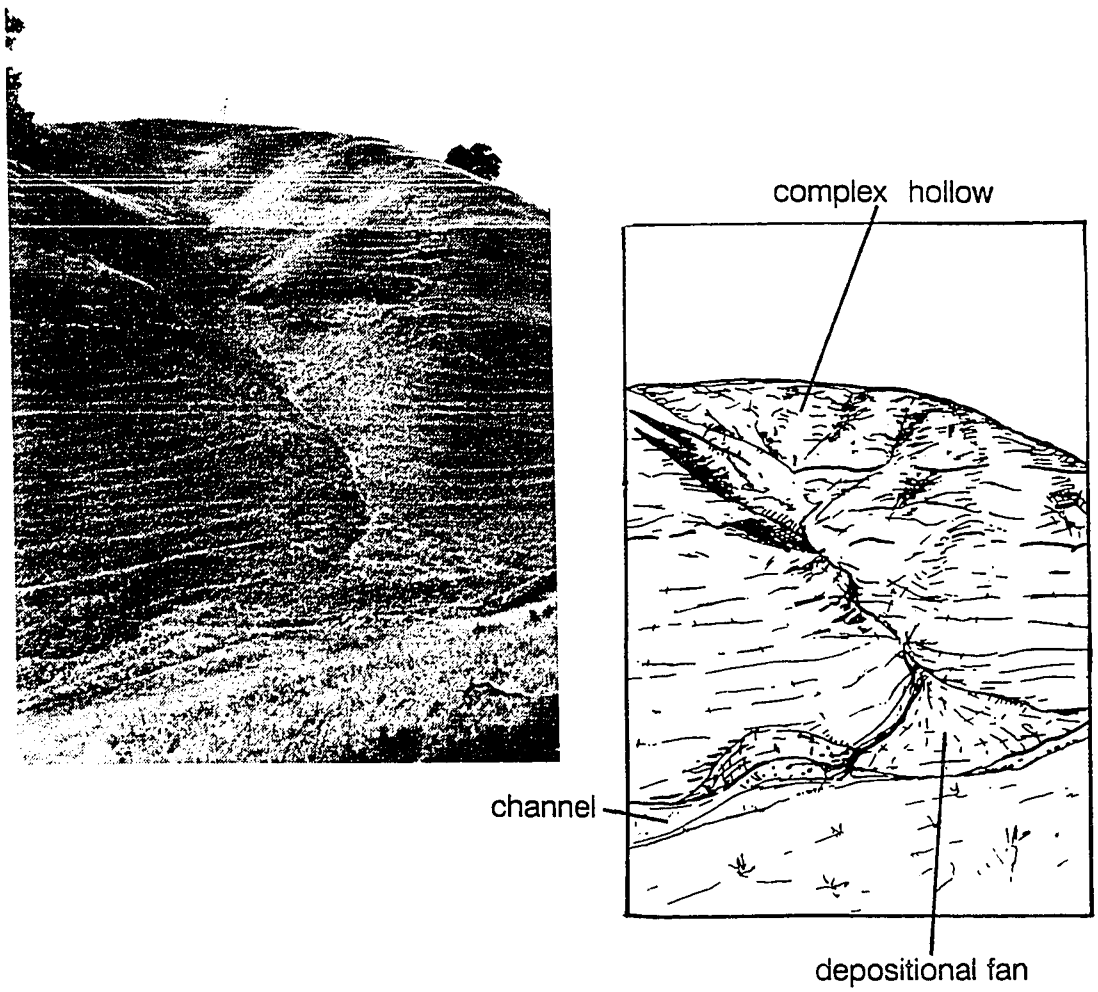

Figure 25. View of a large complex hollow in drainage D2. Hollow is the largest in the study area (same feature as in figure 16).

base of the hollow. The backslopes are concave-out in both axial and plan curvature (fig. 26).

Throughout the area the upper portions of mature hollows have a transition zone where the steep, erosionally active hollow surface intersects the gentler, less active slope segment above, which can be either the upland surface or a section of planar slope. The mouth of the hollow usually is above the channel floor. A depositional fan commonly leads downslope from the mouth to the channel. The fan radiates outward to the adjacent valley walls. These characteristic segments of the hollow can be grouped into three zones, classified by their position along the axial profile of the hollow.

Profile Description

Slope profiles (fig. 27) were measured down the axes of four hollows, which span the ranges of sizes observed in the study area, to allow comparison of their forms. Profiles of adjacent spurs were measured for comparison. Locations of the four profiles are shown on figure 7 and on plate 1. Three distinct zones in the profiles are common to nearly all hollows in the area. Each zone is defined by the primary slope processes and form observed, and each has a characteristic range of slope inclination.

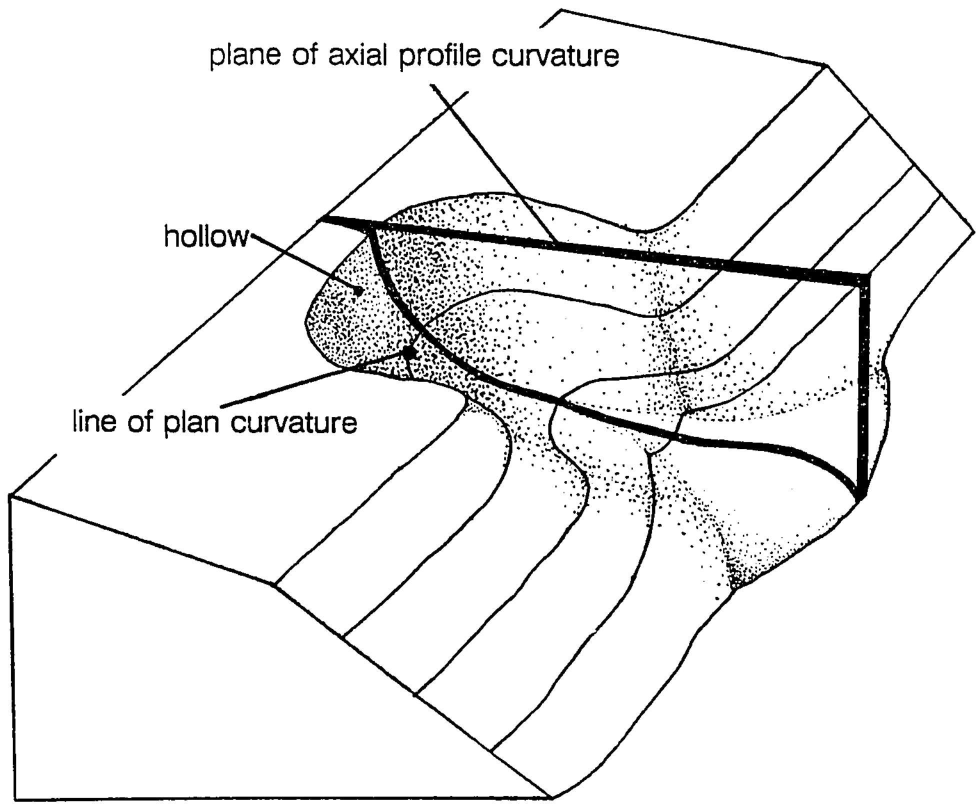

Figure 26. Diagram of hollow geometry, showing relation of axial and plan curvature to hollow form. Curvature is defined as: C=1/r, where r is the radius of the hollow in either plane.

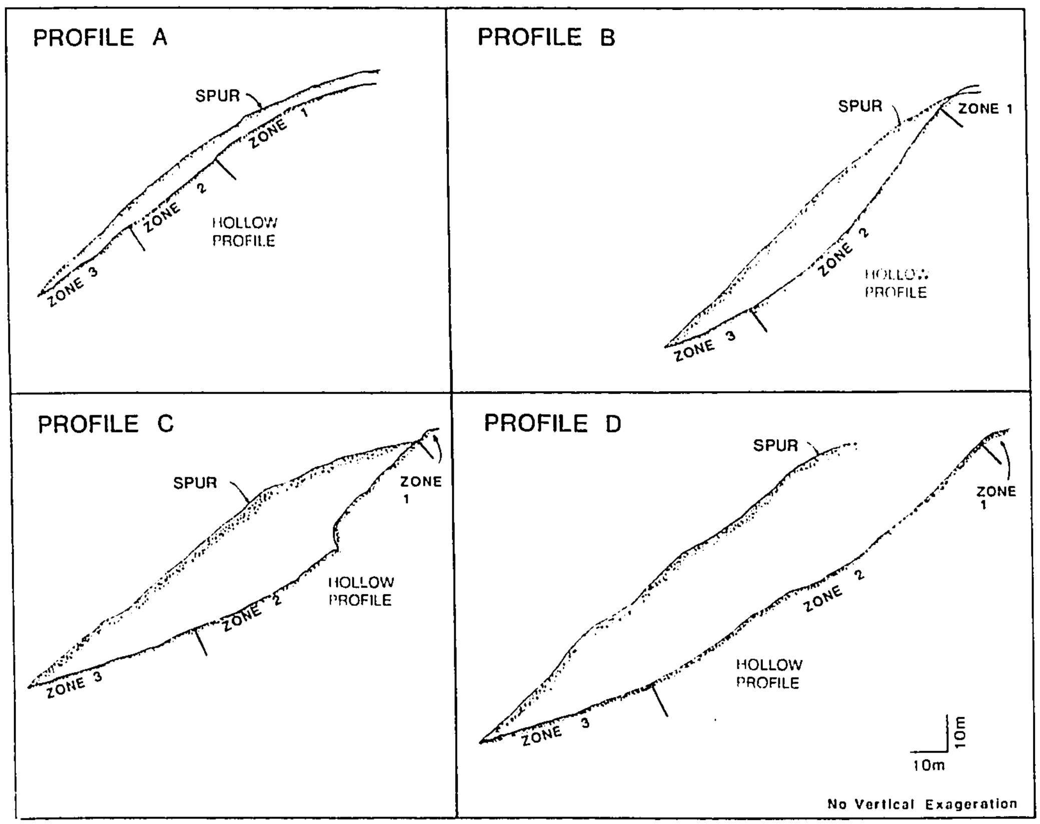

Figure 27. Profiles of spur and hollow axes. Zones are defined and discussed in text. Location of profiles shown on plate 1.

Zone 1 - Transitional Hollow Lip

The uppermost zone (zone 1 in fig. 27) is a gently sloping, rounded section that is convex in profile, located along the upper lip of the hollows. It has a slope inclination ranging from 13 to 36 degrees (average 22 degrees). This relatively low slope angle is related to a well developed, clast-free, argillic horizon more than 1 m thick that is part of the thick terrace soil. This clay-rich soil has adopted a gentler slope angle than the thinner, clast-rich soils developed on the steeper slopes lower in the hollows. The clayey soil appears to be prone to low-rate erosion by rain splash, gravitational creep, and occasional small-scale slumping. The lip of the hollow is a zone of interaction between the fairly stable parts of the hillslope and the erosionally active main hollow.

Zone 2 - Main Hollow

A middle zone within the hollows is straight to broadly concave in axial profile (zone 2 in fig. 27). This zone contains the steepest slopes (40 to 55 degrees), with a slope range of 20 to 55 degrees (average 33 degrees), as well as the greatest concentration of debris-flow scars. Steepness here cannot be attributed to bedrock influence because the same geometry is repeated in hollows located in various parts of the stratigraphic section, as at C and D in figure 7. In plan view, hollows commonly are widest and have the lowest values of curvature in this zone.

Zone 3 - Depositional Area

The zone at the mouth of each hollow (zone 3 in fig. 27) occurs where a relatively gently-sloping depositional fan, with a range in slope of 4 to 25 degrees (average 17 degrees), extends toward the trunk stream (fig. 28). Typically, the distal edge of the fan displaces the creek channel outward (fig. 12).

These fans commonly are small in volume compared to the amount of material eroded from the hollows, indicating that most of the material transported from the hollows has been removed rather than deposited in the fan. Gully incision has progressed from the trunk stream up into the depositional fan areas in a few locations. Only one hollow, however, was identified that contains a gully above the depositional area (fig. 29).

Variations

Variations on the basic hollow form are present in the study area. In several places, hollows are compound features, in which multiple subhollows share a common mouth and depositional fan (fig. 30). Where the lateral

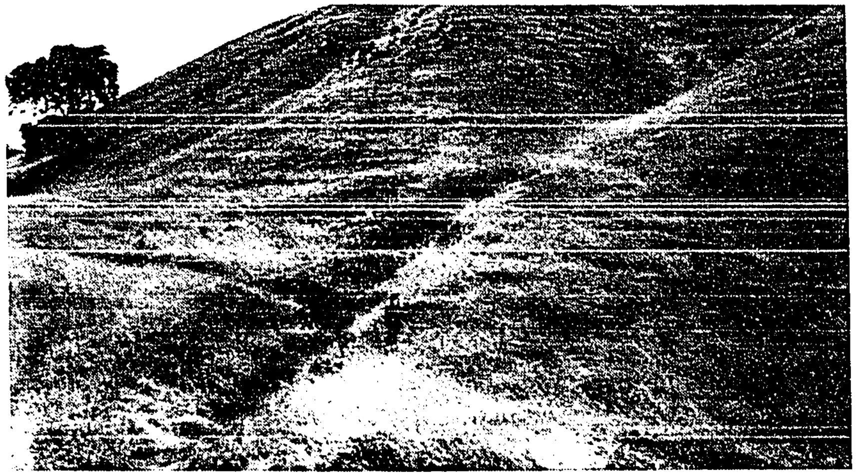

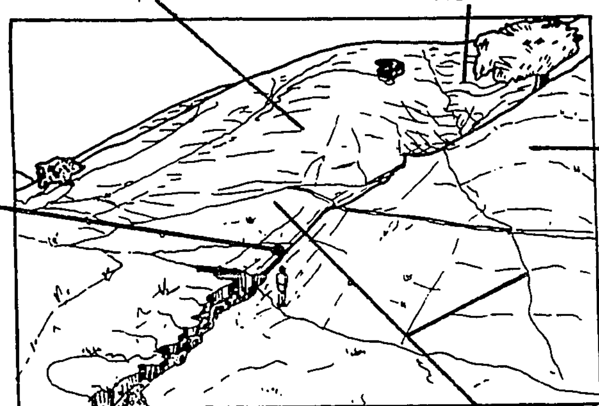

Figure 28. View upslope into the mouth of a medium-sized hollow in drainage D1. The zone 3 depositional fan at the mouth of this hollow has been partially removed by creek erosion on its upstream edge. A small gully has begun to erode into the fan, cutting down to the grade of the creek channel.

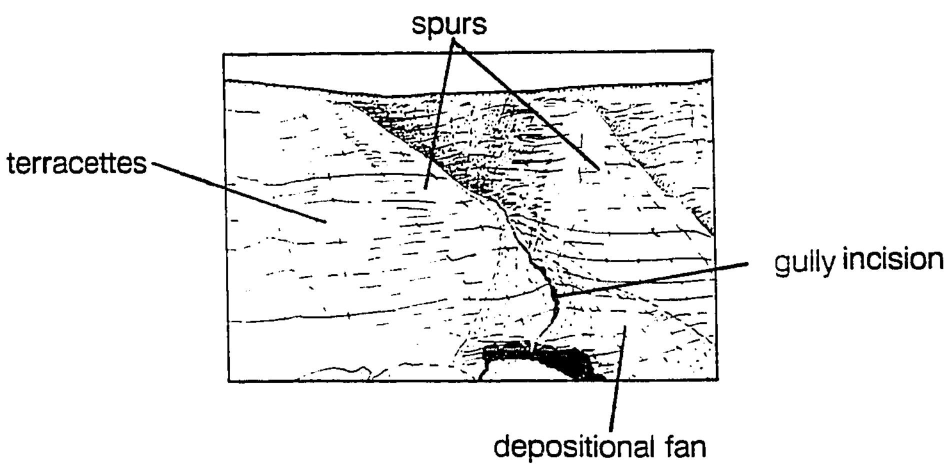

Figure 29. Gully incision in a hollow in drainage D1. The gully extends nearly to the top of the backslope.

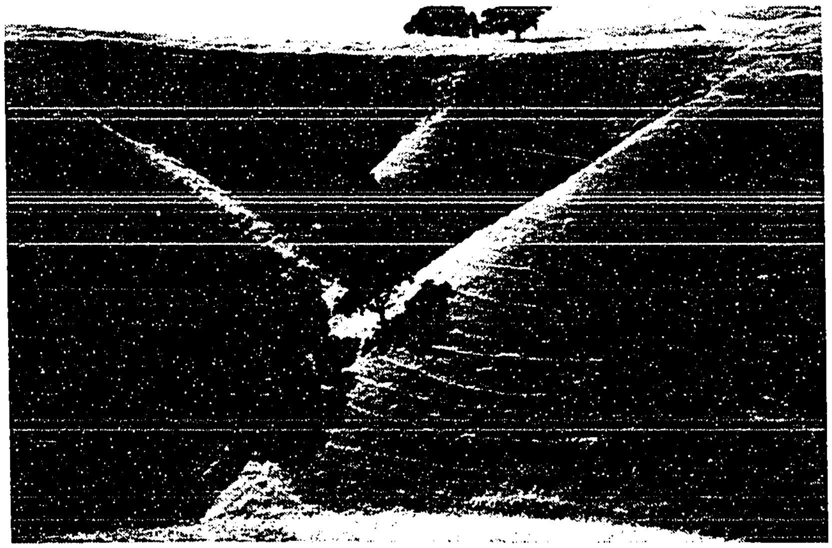

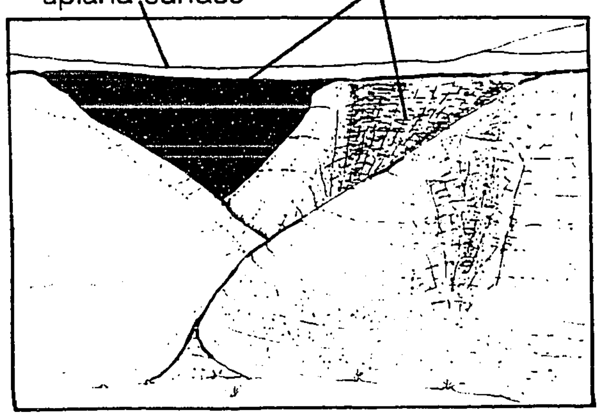

Figure 30. View of a compound hollow in drainage D1, with multiple subhollows sharing a common mouth and depositional fan. Small spur remnants separate the hollows. No incision or channelization has developed.

margins of the enlarging sub-hollows approach each other within the larger hollow, small spurs are left in between. The flow paths from past debris-flow events have joined together downslope to exit the compound hollow in one depositional area.

Where hollows have formed across bedrock outcrops, the basic geometry of the hollow form is maintained (fig. 31). The axial profile C in figure 27 was measured in drainage D1 where the hollow crosses a vertical outcrop estimated to be 4 m high. This profile illustrates how the slope angle and hollow form continue above and below the outcrop.

Slope-inclination Inventory

Angles were measured on upper slope segments around portions of the perimeter of drainage D1 to determine the range of inclination for hollows and spurs. Measurements were made standing on the gently-sloping upland surface looking down along the steeper drainage sidewall. The values of slope inclination are shown in figure 32. The results indicate that slope angles are greater in hollows than on spurs.

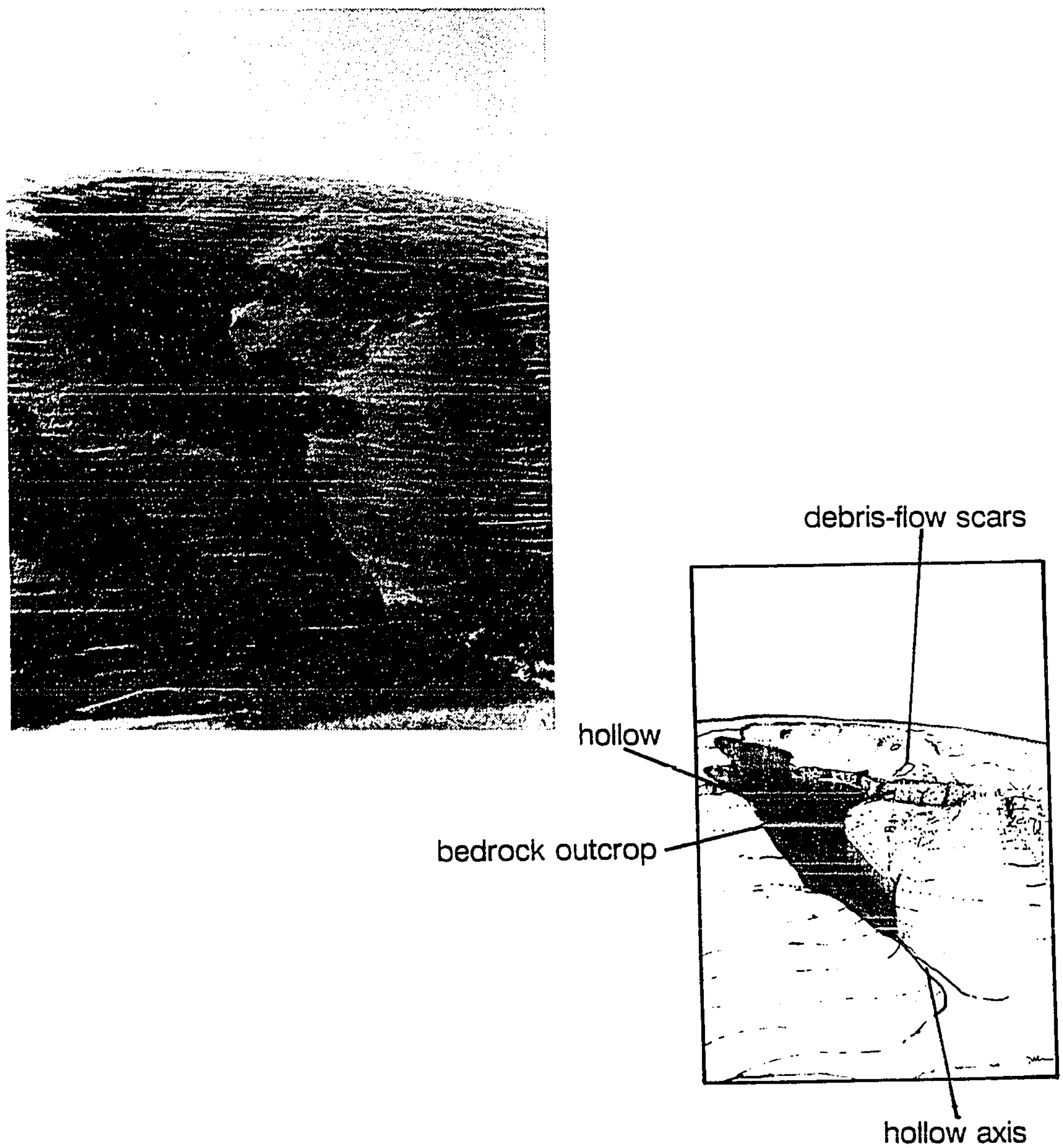

Figure 31. View of a large hollow in drainage D1, that has eroded back through one of the thicker resistant bedrock outcrops. The outcrop forms a zone of nearly vertical slope within the hollow. Scars from recent debris flows are clustered immediately above and below the outcrop. Axial profile C was measured in this hollow.

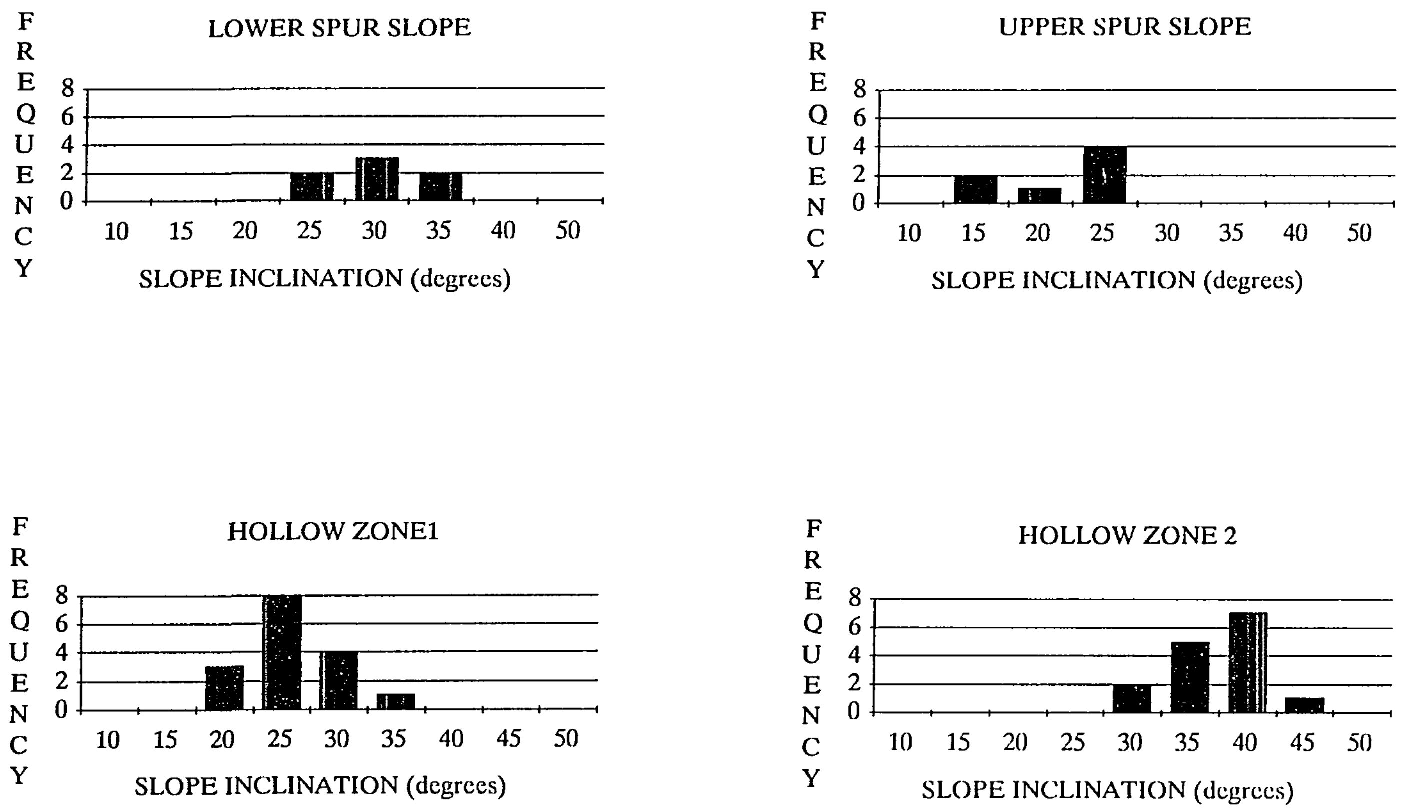

Figure 32. Histogram showing frequency (number of occurrences) of hollow and spur slope inclinations measured along perimeter of drainage D1.

DEBRIS FLOW AND OTHER HILLSLOPE PROCESSES IN THE STUDY AREA

Debris flows are the dominant type of mass movement in the study area. The debris flows observed throughout are similar. This similarity probably can be attributed to the consistent slope angles (fig. 32) and the fairly uniform bedrock lithology and resulting composition of soil and colluvium. Debris flows and scars were observed on the planar slopes as well as in the hollows in the study area. The style of failure and appearance of these debris flows on planar slopes are similar to those of debris flows in the hollows.

Mass movements other than debris flows occur locally in the study area. Small soil slumps are common along the lips of hollows, where clayey upland soils are adjacent to the hollows. These slumps do not develop into debris flows. One earth slide has occurred in a side channel in drainage D2 (plate 1).

Soil Slips and Debris Flows in the Study Area

Eleven debris flows were triggered in the study area during the storm of February 12 to 21, 1986 (table 1, plate 1). Inspection of the fresh features left from these debris flows during the weeks following the storm provided insight into the processes of soil slip and debris flow in this area.

Table 1. DATA ON 1986 DEBRIS FLOWS

DEBRIS FLOW NUMBER	SCAR VOLUME (m3)	SLOPE ANGLE (degrees)	ESTIMATED PERCENT MOBILIZATION	PERCENT CLAY (2um)	PLASTICITY INDEX
1	1.43	10 to 15	<10	13	7
2	2.24	41	100	7	9
3	10.07	41	100	8	7
4	4.83	N/A	90	8	7
5	4.06	31	100	9	6
6	6.63	33	100	13	5
7	16.77	34	100	11	5
8	25.92	31	100	N/A	N/A
9	10.56	<30	80	13	6
10	7.56	33	<50	12	5
11	7.26	N/A	90	9	7

TOTAL VOLUME 97.33 m3

N/A = Not Available

Typical Components

Features of typical soil slip-debris flows observed in the study area are diagrammed in figure 4. Headscarps and flow levees generally have remained recognizable for several years after failure.

Form and Size of Failures

Most scars are sub-rectangular to triangular in shape, with the more pointed part on the uphill side. Head scarps observed soon after failure typically ranged from 25 to 60 cm high and commonly were vertical at the top and rounded at the base. Horizontal lips are common at the lower edge of the scars. Lateral scarps generally decrease slightly in height downslope. Scar sizes range from 2 to 5 m wide and 2 to 8 m long. Scar volumes of the 11 debris flows triggered in the 1986 storm range from 1.4 to 26 m^3.

Mobilization

Soil slips in the area have mobilized into debris flows only at, or downslope from, the contact with the soil developed on the upper terrace surface. The clast-rich, immature soils present below on the steep, incised valley walls and within the hollows fluidize almost completely when they fail, and transform into a flowing slurry of debris (table 1). The ratio of clasts to clay for these hillslope soils (table 2) is such that the minimal amount of fine-grained material

Table 2. SOIL ANALYTICAL DATA FOR SAMPLED DEBRIS FLOWS

LANDSLIDE NUMBER	DATE SAMPLED	DRAINAGE NUMBER	DESCRIPTION and LOCATION	PARTICLE SIZE DISTRIBUTION (mm) gravel >4.76	sand <4.76- >0.075	silt <0.075- >0.002	clay <0.002	ATTERBERG LIMITS LL	PL	PI
1	3/21/86	D1	Slump in upper lip of hollow, sample of head scarp	8	41	38	13	25	18	7
2	3/21/86	D1	Upper of two debris flows in side of hollow, sample of colluvium in sidescarp below terracette	28	43	21	8	29	19	10
2	3/21/86	D1	Head scarp of same debris flow	40	29	24	7	25	16	9
2	3/21/86	D1	Scar floor of same debris flow	52	31	9	8	29	16	13
3	3/21/86	D1	Lower of two debris flows, sample of head scarp	33	42	17	8	25	18	7
4	3/21/86	D1	Debris flow in subhollow of compound hollow, sample of head scarp	22	43	27	8	26	19	7
5	3/21/86	D1	Debris flow in small hollow, sample of head scarp	20	45	26	9	23	17	6
5	3/21/86	D1	Scar floor of same debris flow	34	33	22	11	29	18	11
6	5/29/86	D3	Debris flow on lower slope, sample of head scarp	11	41	35	13	23	18	5
6	5/29/86	D3	Scar floor sample of same debris flow	48	27	15	10	32	20	12
7	5/29/86	D2	Debris flow in shallow hollow, sample of head scarp	17	41	31	11	24	19	5
7	5/29/86	D2	Scar floor sample of same debris flow	27	30	26	17	37	21	16
9	5/29/86	D2	Debris flow low on planar slope, immediately above a resistant outcrop, sample of head scarp	14	40	33	13	24	18	6
9	5/29/86	D2	Scar floor sample of same debris flow	29	35	25	11	24	18	6
10	5/29/86	D2	Small debris flow in narrow hollow, partially-detached block moved 3m, sample of head scarp	25	30	33	12	21	16	5
11	5/29/86	D2	Debris flow in upper portion of large hollow, very fluid mobilization, sample of head scarp	41	29	21	9	25	18	5
11	5/29/86	D2	Scar floor sample of same debris flow, sample hand sorted to remove clasts larger than 6 cm	22	27	33	18	33	19	14

is unable to bind the cobbles into a cohesive mass. The average clay content for 5 of the debris flows that mobilized completely (debris flows 2,3,5,6, and 7 in table 1) is 9.6 percent.

This behavior contrasts with the limited fluidization and mobilization of landslides observed in the cohesive clayey upland soil. Instead of disaggregating and flowing downslope, this material moves intact as much as a few meters downslope, then stops (fig. 33). The greater cohesion of the terrace soil observed in hand samples, coupled with the gentler slope angle, can explain the lack of fluidization of these failures, because the limited shear stresses can not overcome the cohesion of the material even when saturated (Costa, 1984). However, the one debris flow that occurred on the edge of the upland soil during the 1986 storm contained 13 percent clay, but only 10 percent of the mass was mobilized (debris flow 1 in table 1). The limited movement may have been more due to the low slope angle (10-15 degrees) than to higher cohesion. The lack of a thick veneer of cohesive soil in the upper parts of hollows suggests that over time the slumped soil is washed downslope.

Three soil slips triggered during the 1986 storm retained partially-detached portions of soil on the edges of their head scarps, and a soil slip at locality 10 on plate 1 left a substantial soil block intact after moving approximately 3 m downslope. This slide occurred on a 33 degree slope, and left a scarp

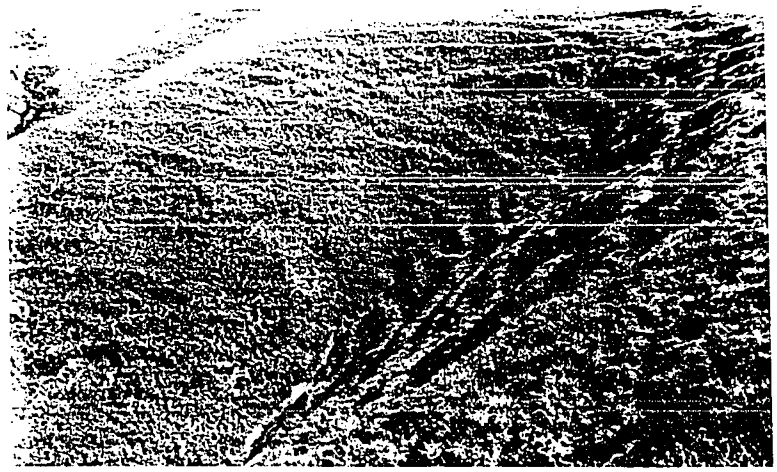

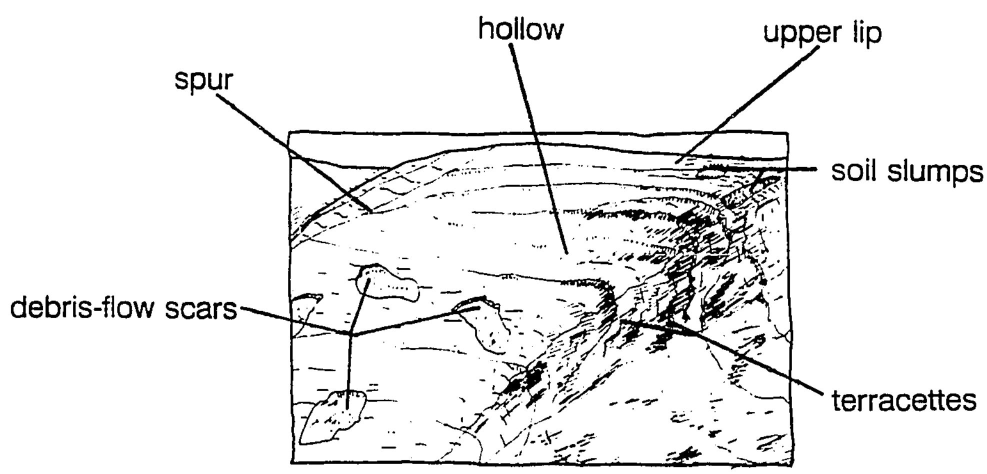

Figure 33. View of the upper lip of a hollow in drainage D1. Arrows point at soil slumps which have failed within the terrace soil, but did not mobilize. The far sideslope has several recent debris-flow scars which occurred in the thinner soils. Stepped terracettes appear in the foreground.

approximately 30 cm high. The margins of the block did mobilize, leaving thick levees on both sides. The head scarp was sampled for material representative of the block, and was determined to have a clay fraction of 12 percent (table 1). This is only 2.4 percent above the average for the sampled soil slips that mobilized entirely, which suggests that other factors prevented mobilization. Several older scars also showed evidence of partial fluidization.

Flow and Scour

Where flow paths could be traced over their entire length, they either extended to the incised channel in the floor of the drainage, or simply tapered out and ended on the slope. The flows generally have not scoured into the ground surface. Figures 34 and 35 show the remains of debris-flow paths within a few weeks of failure. In both cases the grass-covered ground surface is intact and undisturbed beneath the flow. Clumps of grassy sod and matrix-supported gravel clasts form the remnants of lateral levees. In one case, however, scour is evident, as shown in figure 36. Here a second soil-slip scar lies in the path of a debris flow from upslope, suggesting that the flow from upslope raised soil pore pressures or shear stresses enough by scour to trigger the downslope failure.

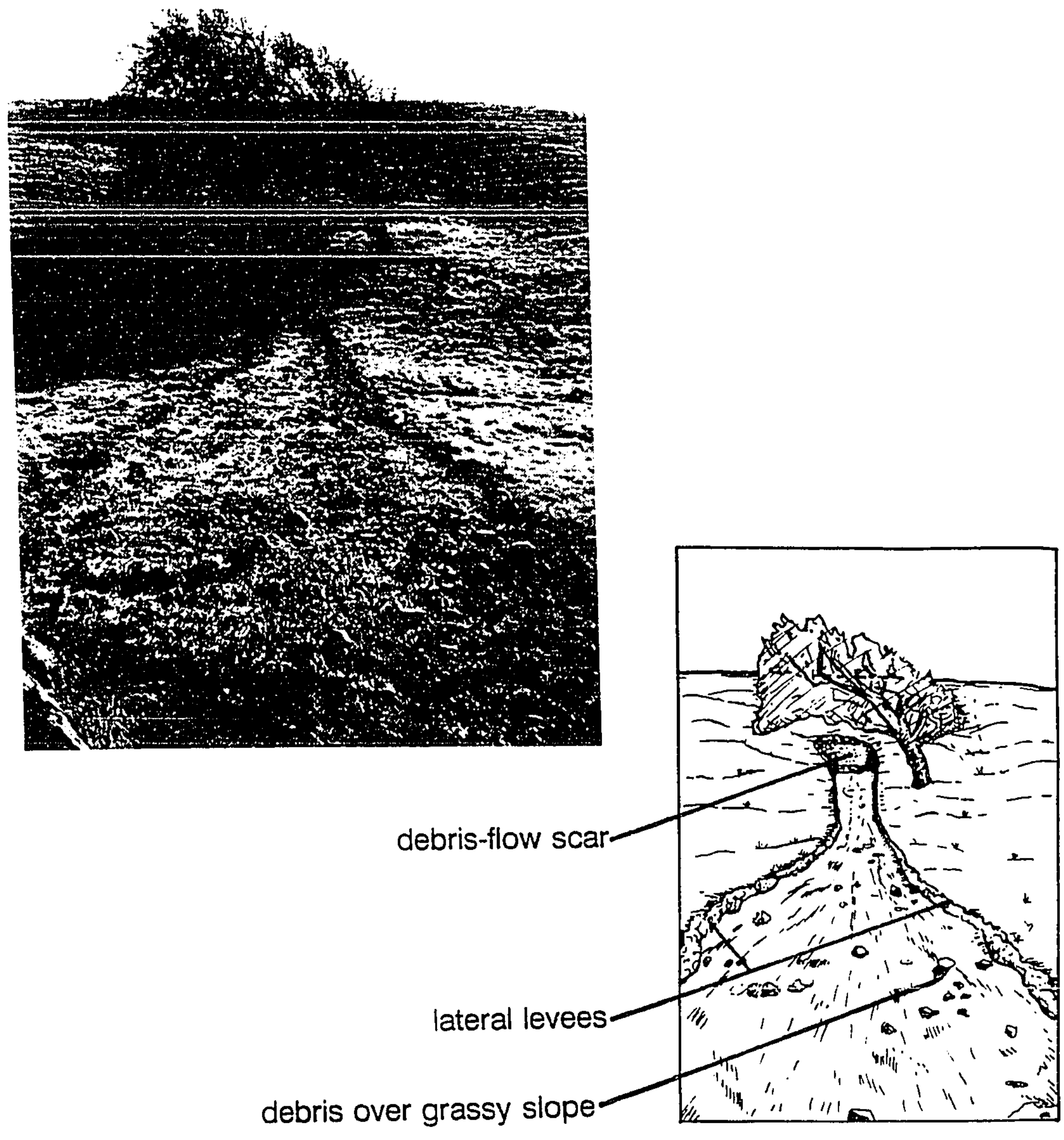

Figure 34. Scar and flow path of a 1986 debris flow. Scar volume was estimated at 8 m^3. Much of the clast-rich debris reached the channel edge just below the bottom of the picture. A discontinuous veneer of debris-flow deposit partially covers the unscoured grassy slope. Lateral levees 10 to 15 cm high consist mostly of fine-grained soil material.

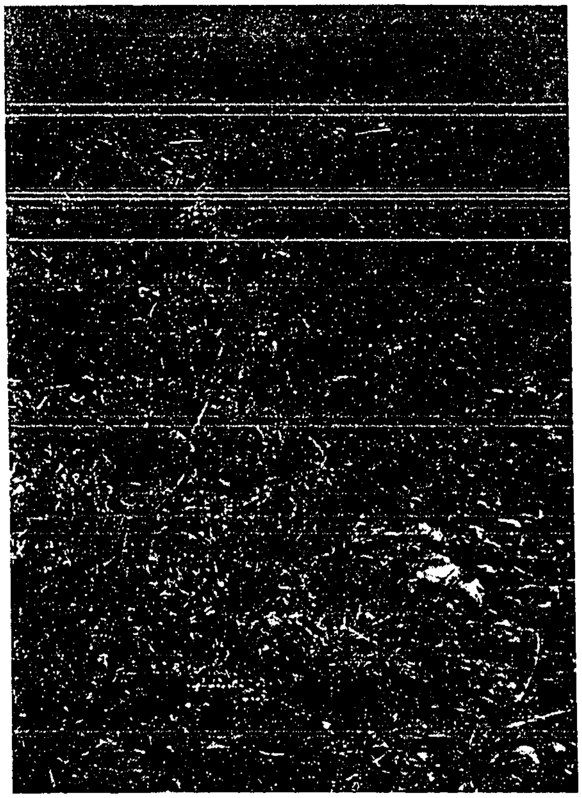

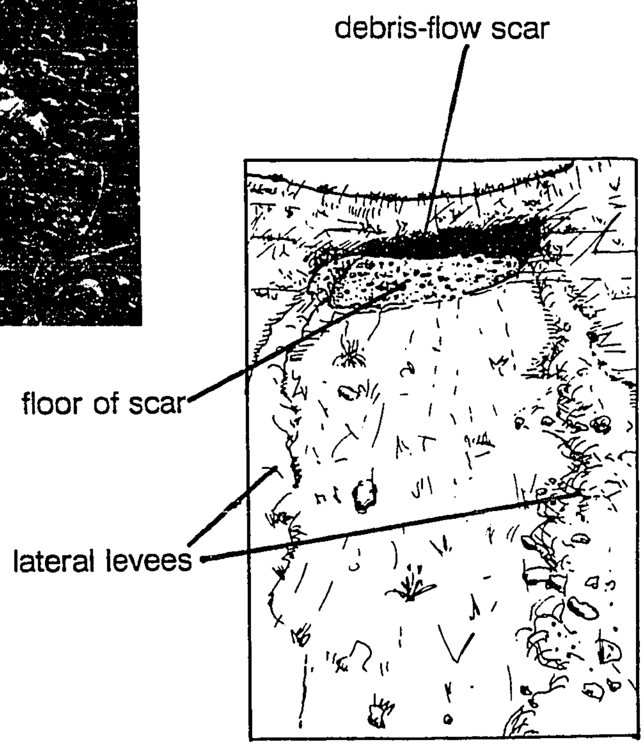

Figure 35. Close-up view of a small 1986 debris-flow scar and flow path one week after failure. The scar is almost completely evacuated down to bedrock. Only the lateral levees remain from the debris that flowed downslope.

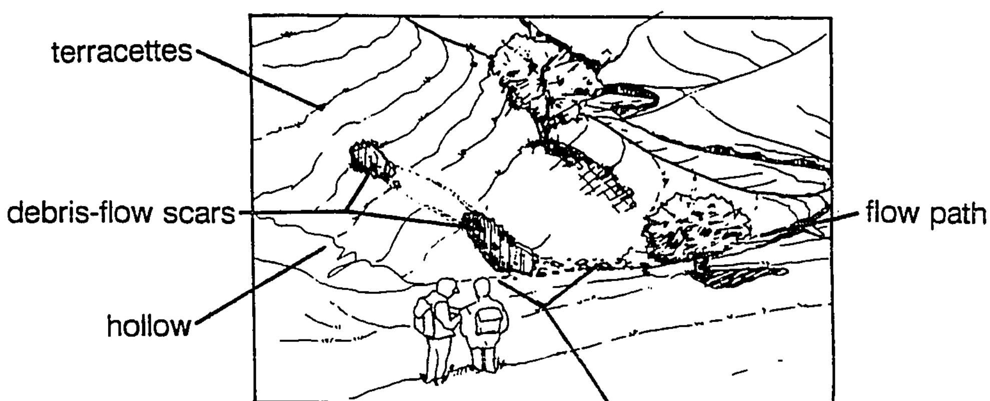

Figure 36. Two debris-flow scars appear as white patches of exposed, weathered bedrock. Both debris flows were triggered during the February 1986 storm and probably represent simultaneous failure. Scour from the upper flow is inferred to have been responsible for initiation of the lower failure.

Water Flow from Scars

All flow paths appear to have experienced flow of water after the debris flow; fresh debris on both the lower scar lips and along the flow paths had been eroded back down to the preexisting grass-covered slope. This evidence of post-failure water flow probably reflects continuing flow of groundwater from the scar. Small-scale gullying was observed along the upper parts of at least two flow paths on slopes that had been observed not to be gullied before the storm.

Scar Weathering and Revegetation

The scars remaining where the failed soil has mobilized generally are evacuated into weathered bedrock (fig. 37). The average soil profile, including weathered bedrock, in the hollows is approximately one meter deep as measured vertically (appendix I), but most head scarps are on the order of 25 to 60 cm high. This leaves an average of a few decimeters of weathered bedrock in the floor of the scars.

Evidence of rapid weathering of the scars was common. The floors of the scars consist of a clayey matrix with coarse pebbles and cobbles of the weathered bedrock. As time progresses after a failure, the coarse material begins to separate from the cohesive matrix, and these loose clasts often move toward the bottom lip of the scar. Revegetation of the scar surface by grasses

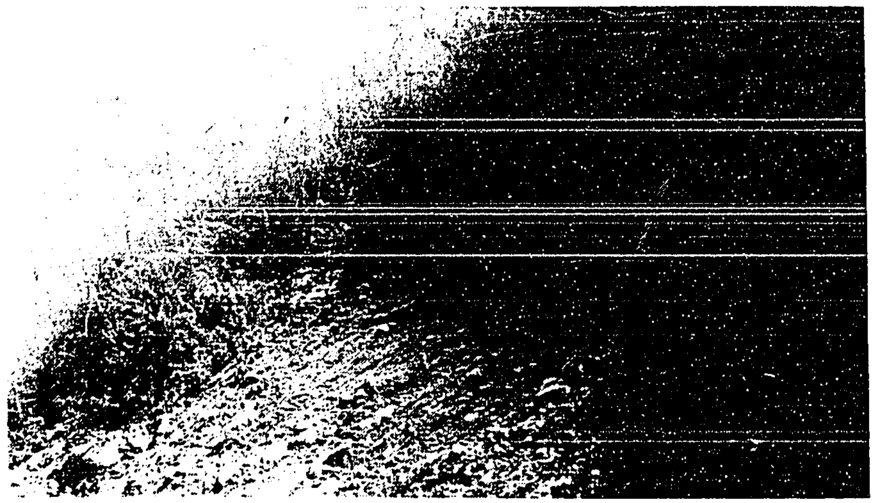

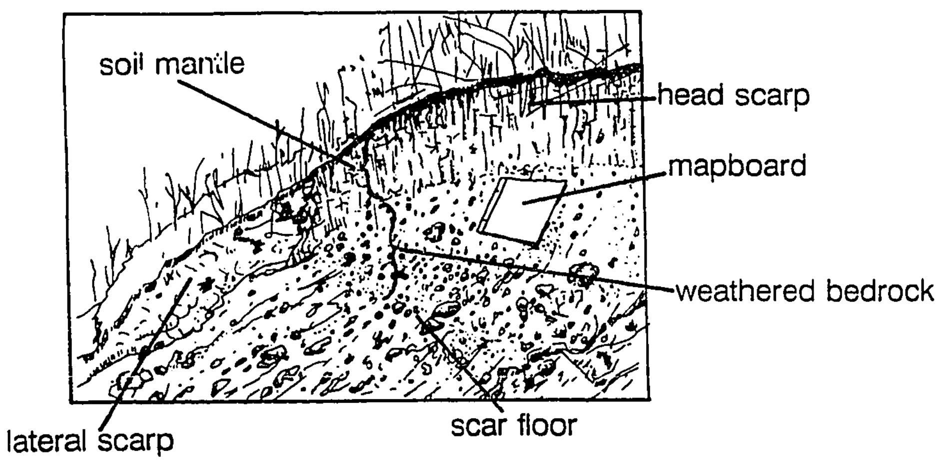

Figure 37. Detail of headscarp of debris-flow scar. Map board is resting on nearly-vertical scarp in soil mantle. Weathered bedrock is exposed in floor of scar.

appears to speed the loosening of the clasts as roots grow between the clasts (fig. 38).

Floors of older scars commonly are covered with loose soil, which has broken free from the upper lip of the scar. Thin soil deposits observed on the terracettes in the hollows (fig. 39) suggest that slopewash may similarly be caught in the scars. Collection of slopewash soil material would enhance the revegetation of the scar. A brief review of aerial photos (table 3) combined with field checking suggests that scars begin to develop a veneer of new soil material approximately 3 to 5 years after failure.

A slightly depressed concavity was observed in the intact soil slopes around several scars, suggesting that subtle small-scale slumping or collapse occurs around the margins of the scars. This depression enhances the visual definition of a beginning hollow shape. Such slumping may enhance the collection of soil debris in the scars.

Channel-bank Failures

Soil slumps also occur along the walls of incised channels toward the head of each drainage (fig. 40). The soil moves directly into the channel, where the debris generally clogs the narrow channel. This kind of failure occurs in the shallowly incised portions of the drainages, and the scars are as long as the

Table 3. AERIAL PHOTOGRAPHS USED IN STUDY

FLIGHT NUMBER	FRAME NUMBER	DATE	SCALE	SOURCE
BUT-281	9, 10	7/26/39	1:12,000	National Archives, Washington, D.C.
AV253-27	54	5/16/57	1:1,000	Pacific Aerial Surveys, Oakland, CA
3072	178, 179	Summer, 1982	1:12,000	National Aeronautics and Space Administration (NASA)

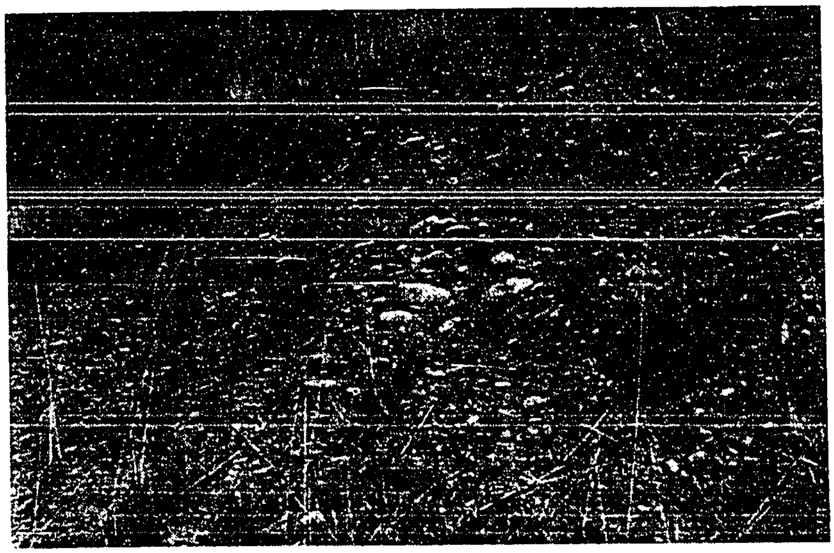

Figure 38. Detail of weathered scar surface. Grasses are becoming re-established in the bedrock as the clayey matrix softens and individual clasts become looser after a few seasons.

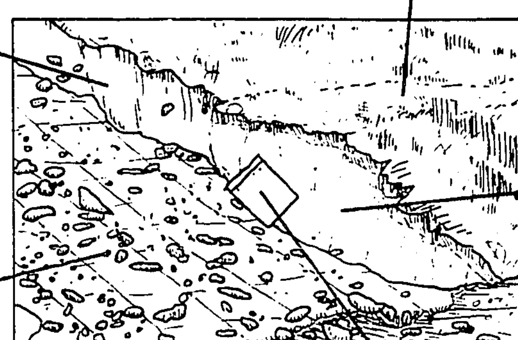

Figure 39. Cross-section of a terracette, showing the variation in thickness of the soil mantle due to compression and displacement of the soil from travel along the path. A veneer of loose colluvium appears just above the map board. Cross-section is the side scarp of a recent debris flow. The scar shows the typical appearance of weathered bedrock.

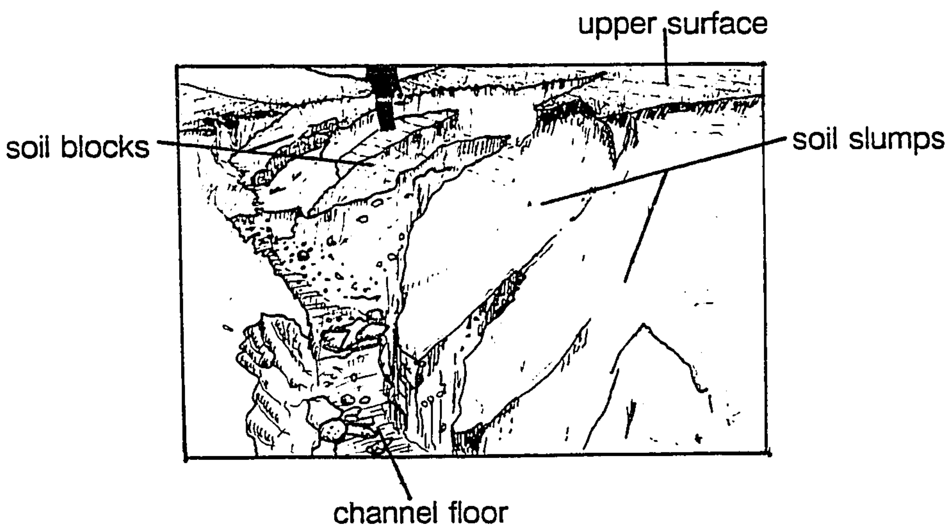

Figure 40. View of the upstream termination of the incised portion of drainage D1. Sidewalls of channel are failing as soil slumps. Nearly the entire sidewall moves during failure.

height of the channel wall. This kind of failure does not occur in the deeply incised parts of the drainages where slope length exceeds scar length.

Inventorying of the individual scars along incised channel walls was difficult due to poor preservation of features. For example, where relief of the channel walls in drainage D1 decreases upstream, soil slips have the appearance of simply widening the channel. Downstream, where relief is greater, the debris-flow scars are shorter than the slope or channel wall and scars are discrete, mappable features. Not enough scars were present to identify the exact transition point along the drainage where slipped soil begins to flow onslope prior to reaching the channel, but it was observed that a slope length of approximately 1.5 times the scar length is needed.

Other Slope Processes

Nearly all hollows become narrower in the downslope direction, where loose clasts and debris commonly litter the less steep axial area. Because nearly all clasts in the soils exhibit a well rounded shape as a result of their alluvial origin, their ability to roll unaided downslope when released may explain the litter. The roundness also may account for the lack of accumulation of clast-rich, unconsolidated material on the upper slopes.

After the February 1986 storm, fresh debris was present at the mouths of nearly all of the hollows, probably as the result of localized overland flow moving material downslope. The debris included small cobbles, disaggregated soil material, and leaf litter (fig. 41). This flushing also appears to assist in the transport of debris previously loosened or mobilized by debris-flow events. In addition, movement of soil and organic material by this flushing could be a primary source of new soil constituents for the scars.

Cattle terracettes are common on all hillslopes in the area (fig. 22). Terracettes are the result of compaction and deformation of the soil mantle by hoofed animals. The terracettes affect the downslope movement of flushed debris by acting as barriers. In addition, the hoofs probably displace soil material downslope during the development of the terracettes.

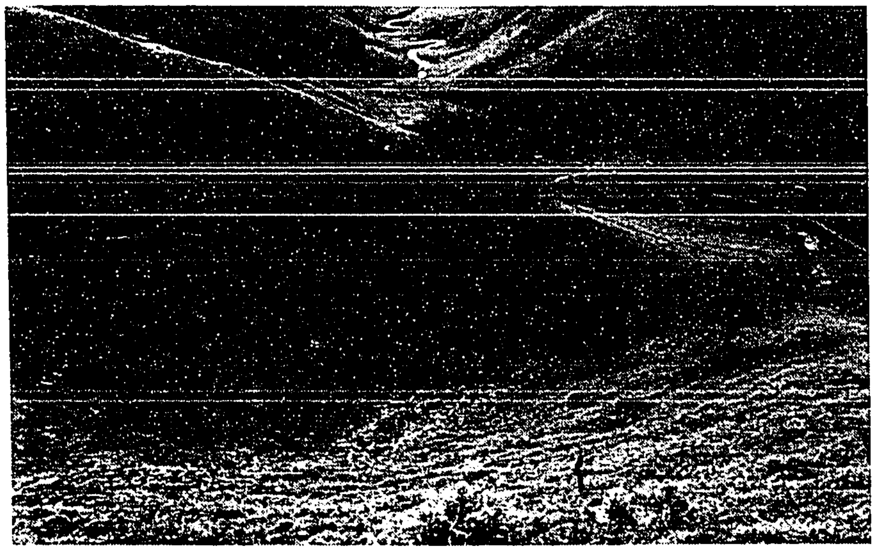

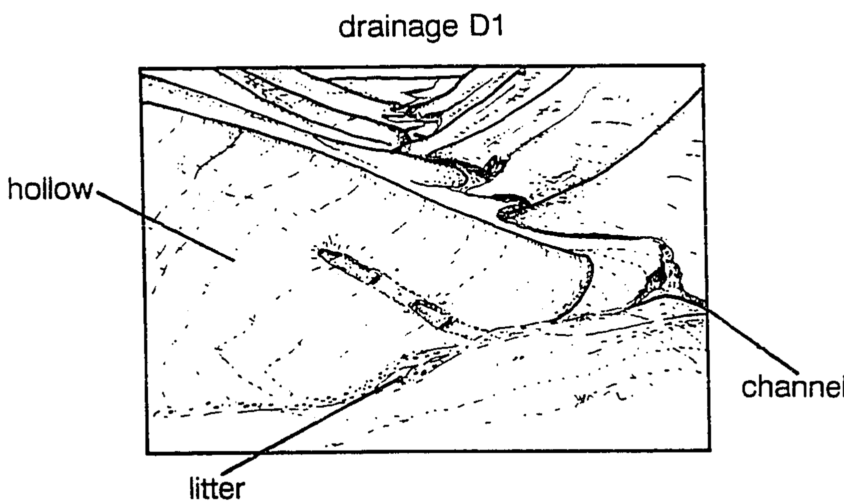

Figure 41. View down towards narrow mouth of hollow. Track of flushed debris is present in hollow axis. Same view as figure 36, within several days of debris-flow event on far slope.

SPATIAL RELATIONSHIPS BETWEEN DEBRIS FLOWS AND HOLLOWS

Debris-flow Occurrence

To determine the spatial relationship between debris-flow scars and hollows, all debris-flow scars visible from the ground and on aerial photographs were plotted on the map of geomorphic features (plate 1). The 272 scars all occurred on steep valley walls. They were classified by their occurrence on either open slopes, spur ridges, or hollows. The results are tabulated in table 4.

In the area as a whole, 74 percent of scars occur in hollows. In D1, the large southern drainage, 94 percent of scars occurred in hollows, as contrasted to 61 percent in the middle drainage, D2, and 57 percent in the smallest, northern drainage, D3. Six to 43 percent of debris flows occur on planar slopes. No debris flows occurred on spurs.

The majority of scars observed occupy the middle to upper portions of hollows. No statistical assessment was made of their occurrence on sidewalls as opposed to backslopes of hollows, but it appears that occurrence is about equally distributed between these areas. A general observation is that scar occurrence is least in the lower portions of the hollows and is greatest in the broad backslope and sidewalls above. The distribution of scars is best shown on plate 1, where in places the symbols lie clustered in arcuate bands.

Table 4. TOPOGRAPHIC POSITION OF DEBRIS-FLOW SCARS

DRAINAGE	D1	D2	D3	TOTAL SCARS AND PERCENTAGES
SCAR LOCATION				
PLANAR SLOPE	6 {6%}	57 {39%}	9 {43%}	72 {26%}
HOLLOW	100 {94%}	88 {61%}	12 {57%}	200 {74%}
SPUR	0 {0%}	0 {0%}	0 {0%}	0 {0%}
TOTAL SCARS	106	145	21	272

[values indicate number of scars in each topographic setting; numbers in brackets indicate percentage of scars represented]

Area of Hollows

Area estimates were made by planimetering the plan (map) view outline of the three main drainages on plate 1, and then planimetering the plan view area of each of the mapped hollows. Because slope inclinations are similar, the plan view area approximates the sideslope area. By comparing the total area for the drainages to the total area for the hollows, the proportion of sideslope area occupied by hollows is quantified. The ratio of the two sets of values represents the percentage of slope occupied by the hollows.

The results (table 5) show that hollows occupy an average of 25 percent of the 3 drainages in the area; individually they occupy 28 percent in D1, 29 percent in D2, and 15 percent in D3. Thus hollows, which occupy an average of only 25 percent of the three drainages, include 74 percent of mapped debris-flow scars, revealing a strong spatial relationship between debris flows and hollows.

Table 5. AREAS AND AREA PERCENTAGES

DRAINAGE NUMBER	D1	D2	D3	TOTAL FOR 3 DRAINAGES
DRAINAGE (PLAN VIEW) AREA (m2)	96,767	95,060	50,526	80,784
HOLLOW (PLAN VIEW) AREA (m2)	26,767	27,516	7,513	20,599
PERCENTAGE OF HOLLOW PLAN VIEW AREA IN DRAINAGE PLAN VIEW AREA	{28%}	{29%}	{15%}	{25%}

GENETIC RELATIONSHIP BETWEEN DEBRIS FLOWS AND HOLLOWS

Sufficiency of Debris-flow Processes

Debris flows appear to be the dominant slope process now occurring in the study area, and they are spatially concentrated in hollows. To learn if debris flows over time could have carved the hollows, it must be determined what time period would be required to transport all of the material from the hollows. This question can be addressed by comparing the quantity of material removed by debris flows during a single storm of known recurrence to the estimated volume removed over time from the hollows. This calculation assumes that the incised drainages existed prior to the initiation of hollows or that the removal that formed the drainages was by processes other than debris flow.

Approach

Storm recurrence intervals represent the statistical likelihood of the time interval in which a storm of given magnitude will occur. If a storm of given magnitude triggers debris flows, then over the long term, it can be inferred that a similar number of debris flows will be triggered by storms of this magnitude during each recurrence interval. By multiplying the volume of material removed during such storms by the recurrence interval, the cumulative erosion potential of many equivalent storms can be determined and used to estimate the amount of time required to erode the hollows by repeated storms of this same recurrence interval.

A rough, order-of-magnitude calculation of erosion by debris flows was based on an estimated recurrence interval for the debris-flow producing storm of 12 to 21 February 1986. Rainfall information from the raingage (location shown on figure 1) is presented in table 6. Using the methods of Rantz (1971), a recurrence interval of 11 years was calculated for the 7-day, high-rainfall segment of the storm. Eleven debris flows were triggered during the storm (plate 1), and these moved 97 m^3 of soil from the hillslopes (table 1), either down into the main channel or onto the fans.

Volume

Hollow volumes were estimated by first planimetering the area represented by enclosing each of the topographic contour lines and then multiplying by their contour interval to approximate the total drainage volumes. The actual topography, including the hollows, is represented on the map by crenulations in the contours. By sketching a straight line across each of the crenulations and connecting it to the contour line on either side, as shown in figure 42, the now straightened contour lines smooth the topographic shape of the drainage slopes and remove the crenulations in the contour lines that portray the hollows.

Table 6. 1986 STORM DATA

DAILY PRECIPITATION TOTALS FOR 1986 STORM IN STUDY AREA (data from San Francisco Water Department guage located at San Antonio Reservoir Dam)

DAY	CM	IN
12-Feb	0.20	0.08
13-Feb	1.24	0.49
14-Feb	1.19	0.47
15-Feb	5.31	2.09
16-Feb	0.97	0.38
17-Feb	1.80	0.71
18-Feb	2.21	0.87
19-Feb	5.84	2.3
20-Feb	0.25	0.1
21-Feb	0.03	0.01
TOTAL STORM PRECIPITATION	19.05	7.5

MEAN ANNUAL RAINFAL 52.07 cm (20.5 in)

MAIN STORM DURATION

7 days for total from 2/13-2/19

5 days for lesser total from 2/15-2/19

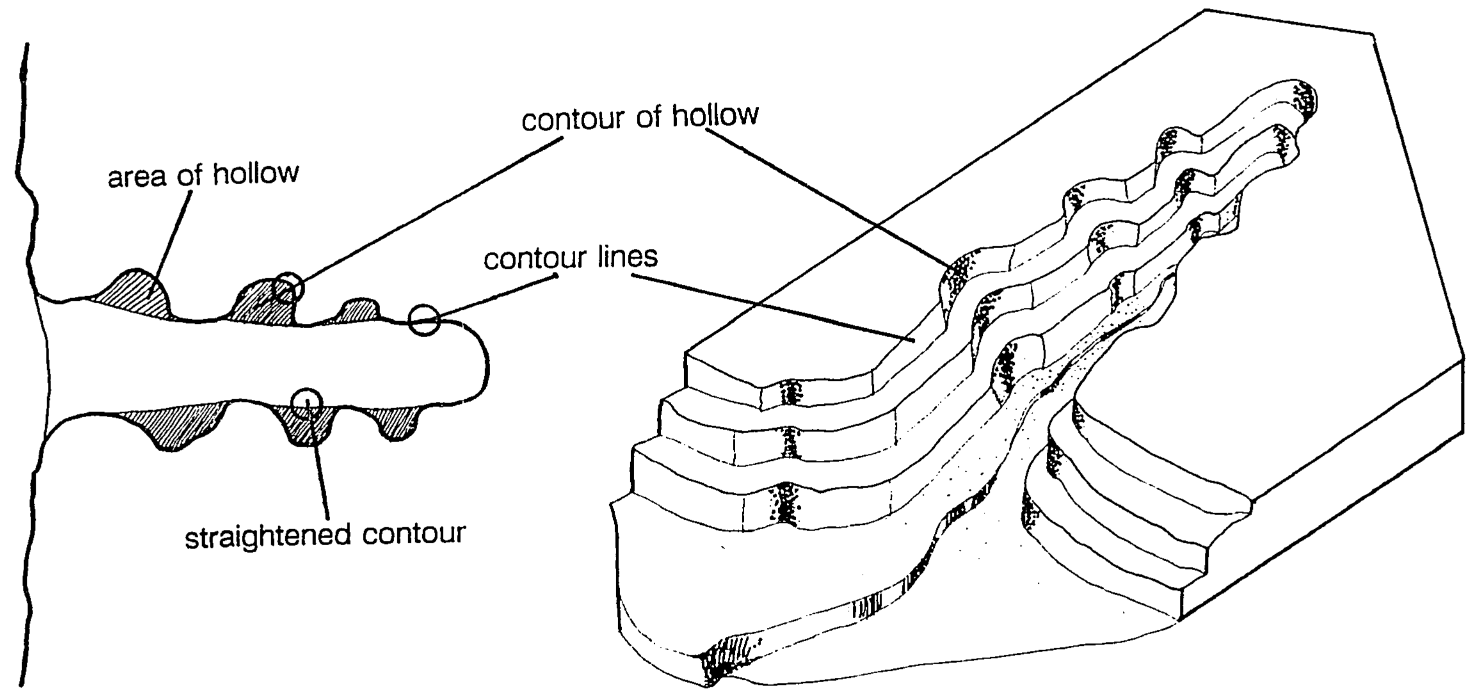

Figure 42. Contour lines were used as indicators of slope length and height in order to estimate the approximate volumes of hollows. Perspective sketch demonstrates volumetric representation of topography by contour lines. Shaded pattern represents hollow areas delineated by straightening crenulated contour lines.

Existing and modified contours in each drainage were planimetered to determine the areas of each interval. These areas were then multiplied by the contour interval to approximate the volumes of a drainage both with and without hollows (table 7). Subtracting the modified volumes from the true volumes gives an estimate of the total hollow volumes for all three drainages of approximately 45,000 m^3.

Erosion Rates

The 45,000 m^3 estimated volume of the hollows (table 7) was divided by the 97 m^3 of soil moved by debris flows in the February 1986 storm. The results represent an estimate of the number of equivalent storm events needed to carve the hollows from planar hillslopes. Multiplying by the 11-year recurrence interval shows that a time period of approximately 5,000 years is sufficient to carve the hollows by storms of this magnitude.

Rates of debris-flow erosion probably were lower in earlier stages of development, when fewer steep slopes existed in the area. On the other hand, storms of different magnitude and return intervals surely also trigger debris flows in the area, thereby increasing the rate of hollow development over that from 11-year storms alone. Thus, although uncertainties are substantial, it appears reasonable that rates of debris-flow erosion are sufficient to have

Table 7. VOLUME CALCULATIONS

DRAINAGE D1

ACTUAL CONTOURS

reference contour	height (m) of contour interval		cross-sectional area (m2) from planimeter reading:		volume (m3) of contour interval
480	12.19	X	7,093	=	86,478
440	12.19	X	5,630	=	68,641
400	12.19	X	3,154	=	38,454
360	12.19	X	1,373	=	16,740
320	12.19	X	397	=	4,840

TOTAL DRAINAGE VOLUME FOR ACTUAL CONTOURS: 215,000 m3

SMOOTHED CONTOURS

reference contour	height (m) of contour interval		cross-sectional area (m2) from planimeter reading:		volume (m3) of contour interval
480	12.19	X	6,699	=	81,674
440	12.19	X	5,110	=	62,301
400	12.19	X	2,813	=	34,296
360	12.19	X	1,209	=	14,740
320	12.19	X	340	=	4,145

TOTAL DRAINAGE VOLUME FOR SMOOTHED CONTOURS: 197,000 m3

ESTIMATED HOLLOW VOLUME = ACTUAL CONTOUR VOLUME - SMOOTHED CONTOUR VOLUME:

215,000 m3 - 197,000 m3 = 18,000 m3

Table 7. VOLUME CALCULATIONS
CONTINUED

DRAINAGE D2

ACTUAL CONTOURS

reference contour	height (m) of contour interval		cross-sectional area (m2) from planimeter reading:		volume (m3) of contour interval
520	12.19	X	1,140	=	13,899
480	12.19	X	4,940	=	60,228
440	12.19	X	4,480	=	54,620
400	12.19	X	2,293	=	27,956
360	12.19	X	1,136	=	13,850
320	12.19	X	240	=	2,926

TOTAL DRAINAGE VOLUME
FOR ACTUAL CONTOURS $\boxed{175{,}000 \text{ m3}}$

SMOOTHED CONTOURS

reference contour	height (m) of contour interval		cross-sectional area (m2) from planimeter reading:		volume (m3) of contour interval
520	12.19	X	1,007	=	12,277
480	12.19	X	4,503	=	54,901
440	12.19	X	3,957	=	48,244
400	12.19	X	2,015	=	24,567
360	12.19	X	980	=	11,948
320	12.19	X	184	=	2,243

TOTAL DRAINAGE VOLUME
FOR SMOOTHED CONTOURS $\boxed{154{,}000 \text{ m3}}$

ESTIMATED HOLLOW VOLUME = ACTUAL CONTOUR VOLUME - SMOOTHED CONTOUR VOLUME:

$\boxed{175{,}000 \text{ m3} - 154{,}000 \text{ m3} = 21{,}000 \text{ m3}}$

Table 7. VOLUME CALCULATIONS
CONTINUED

DRAINAGE D3

ACTUAL CONTOURS

reference contour	height (m) of contour interval		cross-sectional area (m2) from planimeter reading:		volume (m3) of contour interval
520	12.19	X	2,783	=	33,930
480	12.19	X	1,977	=	24,104
440	12.19	X	1,173	=	14,301
400	12.19	X	496	=	6,047
360	12.19	X	167	=	2,036
320	12.19	X	52	=	634

TOTAL DRAINAGE VOLUME FOR ACTUAL CONTOURS: 81,000 m3

SMOOTHED CONTOURS

reference contour	height (m) of contour interval		cross-sectional area (m2) from planimeter reading:		volume (m3) of contour interval
520	12.19	X	2,587	=	31,541
480	12.19	X	1,821	=	22,202
440	12.19	X	1,076	=	13,119
400	12.19	X	435	=	5,304
360	12.19	X	154	=	1,878
320	12.19	X	52	=	634

TOTAL DRAINAGE VOLUME FOR SMOOTHED CONTOURS: 75,000 m3

ESTIMATED HOLLOW VOLUME = ACTUAL CONTOUR VOLUME - SMOOTHED CONTOUR VOLUME:

81,000 m3 - 75,000 m3 = 6,000 m3

TOTAL HOLLOW VOLUME FOR ALL THREE DRAINAGES: 45,000 m3 carved the hollows, without contributions from other slope processes, within about 5,000 years.

Climatic Constraints

Climatic constraints, such as yearly rainfall and storm patterns, are known to influence slope processes (Carson, 1980). If these constraints are constant during a climatic period, then their influence on slope processes should also be constant. One check on whether debris flows appear to be sufficient to carve the hollows in the study area is to determine whether climate has been constant for the approximately 5,000 years required. Johnson (1977) has determined from paleoecologic studies that the climate in the San Francisco Bay area has been fairly stable for the duration of the Holocene, a period of 10,000 years, permitting adequate time for formation of the hollows by debris flows.

Continuum of Hollow Size and Continuity of Process

A continuum of hollow sizes is exhibited in the study area, and this appears to represent stages in the evolutionary sequence of hollow development. No evidence has been found that processes of hollow erosion other than debris flow have been important in the past. Although there is a strong contrast between the old landscape and the hollows, there is no evidence for discontinuity in stages of hollow development. If different processes had been significant in hollow development, some shapes other than those seen today should be apparent.

In summary, the present-day process of debris flow occurring in the study area is spatially related to hollows, and debris flows appear capable of erosion at a rate sufficient to have carved the hollows during the Holocene. Further, the continuum of hollow forms in the study area suggests that only one dominant process has acted on the hillslopes over time. Together, these lines of evidence suggest that debris flows are responsible for the development of the hollows.

HOLLOW INITIATION AND DEVELOPMENT

Because of the number of debris-flow scars and the continuum of hollow size and shape, the study area provides a favorable setting for the development of a descriptive model of initial hollow formation from debris-flow events. This section identifies the key aspects of debris flows and presents a model for the initiation and enlargement of hollows.

Field observations of scars shown on plate 1 suggest that a direct relationship exists between individual debris-flow events and the initiation of hollow forms. Because landslides that occur within hillside soils in the study area nearly always undergo mobilization and flow away from their source, the most distinctive feature visible afterwards is the evacuated scar left on the hillslope. Mapping of the scar locations suggests that the scars are randomly scattered where slope length is small enough to limit the runout distance from lower scarp to base of slope. Scars appear to cluster where slope length and inclination are great enough to allow flow away from the scar, which results in isolation of the scar from the valley floor (plate 1).

The slope length controls whether the deposit of debris remains onslope, where it affects future slope processes by buttressing, or flows off-slope into the active channel (fig. 43). An example of the lower limit of slope length would be a scar of length equal to the length of slope on which it occurred. At this extreme, the material can only slump into the channel without isolating the scar

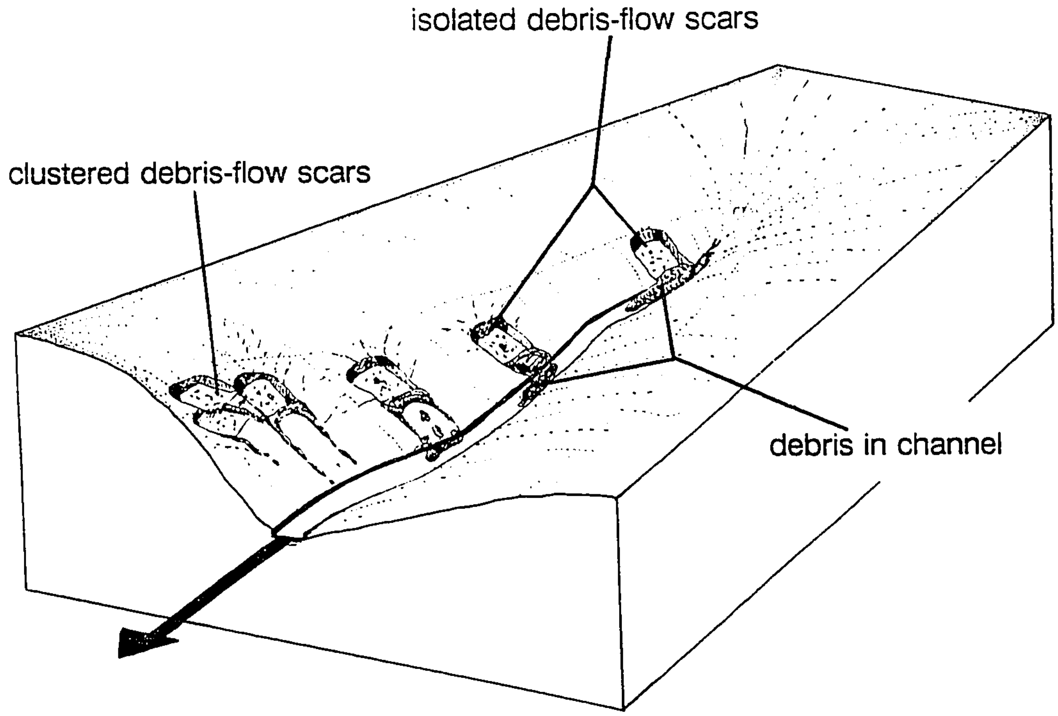

Figure 43. Diagram of the relationship of slope relief to isolation of debris-flow scars from channel. Clustering of scars leads to development of incipient hollow forms.

from its slide debris. Below this extreme, the slumped debris buttresses the slope and clogs the scar, which then dampens the possibility of further failure at this point.

Spatial clustering of scars becomes apparent where slope length is great enough to allow onslope mobilization (plate 1). The upstream, headward portion of drainage D2 best demonstrates this relationship. Figure 43 illustrates the scar patterns related to incipient hollow forms.

Hollow Initiation

The initiation of the hollow-forming process apparently begins with the occurrence of single debris flows isolated from the channel. When additional debris flows occur close to the original scar, the proto-hollow form is initiated.

Debris flows can occur anywhere within the soil mantle on the drainage side slopes. To estimate the length of slope necessary to allow isolation of the debris flow from the channel, it is assumed first that landslide scars have a constant length, so that slope length can be measured in units of scar length. A factor is also needed to address the length of slope required to allow complete mobilization of the soil as it slips from the scar. A factor of one-half the scar length, based on observations of soil slips in the low-relief channels, has been used.

The model begins with the slope length equal to scar length. At this stage, each time a landslide occurs, the failed material will slump into the active channel, where it ultimately will be mobilized or eroded and transported downstream. The net effect on the slope, as sketched in figure 44 (case A), will be to widen the channel. No erosion is concentrated at any single point on length of the slope; rather, the entire downslope length is simultaneously eroded.

The next step in the model is a threshold situation, in which slope length is equal to the length of slope needed for mobilization, which is estimated to be 1.5 times the scar length (fig. 44, case B). At this point, the scar begins to be isolated from the channel, but still focuses the erosion near the base of the slope.

The third step can occur when slope length is great enough to allow complete mobilization of the debris, and transport of the flowing material away from the scar. At this point, the scar can be completely separated from the active channel processes (fig. 44, case C).

Hollow Enlargement

Once a scar appears on the model hillslope, it will become a new factor affecting the hydrologic flow regime. Localized removal of the soil mantle can

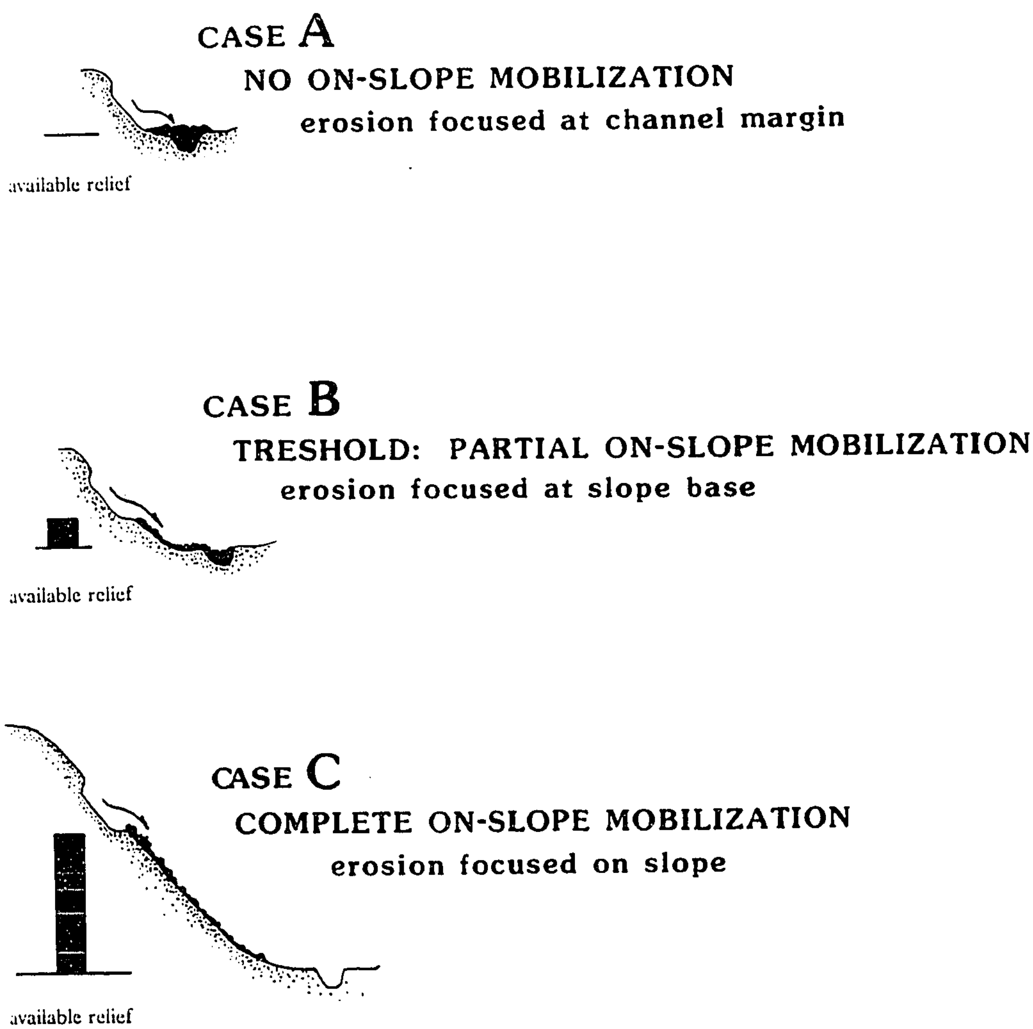

Figure 44. Diagram of three cases relating the impact and location of slope erosion by debris flows to the amount of slope relief.

cause near-surface flowlines to be drawn towards the more permeable scar face (Kirkby, 1987; Reid and others, 1988). By concentrating groundwater flow near the scar, the potential for enhanced saturation and positive pore pressures increases. The scar will also lead to dilation of the surface soils as they relax towards the open head and side scarps. These conditions enhance the potential for further failure, so that landsliding events will preferentially occur near the previous scar rather than randomly on the hillslope. Continuation of this process leads to the further definition of the hollow form and its subsequent enlargement.

CONCLUSIONS

Mapping of debris-flow features in the Sunol study area, combined with description of geomorphic forms, has indicated that debris flows are the dominant form of erosion on hillslopes in this area. The debris flows occur more commonly within the hollows rather than on planar slopes and spurs. Of the 272 debris-flow scars mapped, 74 percent occur in the hollows, compared to 26 percent on planar slopes and none on spurs. This spatial association suggests that hollows and debris flows are genetically related.

Removal of the soil mantle and, to a lesser degree, of weathered bedrock, by debris flows appears to lead to initial formation and enlargement of the hollows. Once formed, the hollows inherently affect conditions that increase the likelihood that debris flows will occur within the area of the hollows.

Estimates of rates of removal of slope material suggest that debris flows are sufficient to have carved the hollows within the Holocene, without substantial contribution from other hillslope processes. The continuum of hollow sizes and shapes, in combination with a record of constant climate over the Holocene, suggests that the process of debris flow that is evident today operated similarly in the past to carve the hollows.

These lines of evidence suggest that hollows in this landscape form by debris flow and enlarge by concentrating the occurrence of debris flows. A model of hollow development, based on observations in the study area, suggests that hollows may develop once a threshold in local relief is reached in the drainage during stream incision, and that they will continue to develop as long as debris-flow-triggering conditions exist.

The hollows formed in the Sunol study area appear to record the long-term impact of debris flows on this landscape. Most importantly, they are forming from processes other than those that are responsible for development of the first-order drainages. This has broader importance because the hollows appear to demonstrate early stages of drainage basin development in the study area. As a consequence of their initiation and enlargement, the hollows are eroding away the planar slopes that represent the original slopes of the drainages and may, in time, lead to changes in the overall drainage pattern.

Future work in this area could consider the remaining questions of how the present drainages were formed, and how they might evolve in the future as a result of changes in tectonic and climatic settings. An integral part of any further work would be to estimate the impact of enlargement of the existing hollows on the evolution of the overall basin morphology.

REFERENCES CITED

Barlock, V. E., 1989, Sedimentology of the Livermore Gravels (Miocene-Pleistocene), southern Livermore Valley, California, [M.S. thesis]: San Jose State University, San Jose, 110 p.

Beverage, J.P., and Culbertson, J.K., 1964, Hyper-concentrations of suspended sediment: American Society of Civil Engineers, Hydraulic Division Journal, no. HY6, p. 117-126.

Burford, R.O., and Sharp, R.V., 1982, Slip on the Hayward and Calaveras faults determined from offset powerlines: California Division of Mines and Geology Special Publication 62, p. 261-269.

Carson, M.A., 1980, Mass-wasting, slope development and climate, in Derbyshire, E., ed., Geomorphology and climate: John Wiley and Sons, London, p. 101-136.

Clark, B.L., 1930, Tectonics of the Coast Ranges of middle California: Geological Society of America Bulletin, v. 41, p. 747-828.

Costa, J.E., 1984, Physical geomorphology of debris flows, in Costa, J.E., and Fleisher, P.J., eds., Developments and applications of geomorphology: Springer-Verlag, Berlin, p. 268-316.

Costa, J.E., and Wieczorek, G.F., eds., 1987, Debris flows/avalanches: process, recognition, and mitigation: Geological Society of America, Reviews in Engineering Geology, v. 7, 239 p.

Dibblee, T.W., Jr., 1980, Preliminary geologic map of the La Costa Valley quadrangle, Alameda County, California: U.S. Geological Survey Open-file Report 80-533, sheet 1, scale 1:24,000.

Dietrich, W.E., Reneau, S.L., and Wilson, C.J., 1987, Overview: "zero-order basins" and problems of drainage density, sediment transport and hillslope morphology, in Beschta, R.L., Blinn, T., Grant, G.E., Ice, G.G., and Swanson, F.J., eds., Erosion and sedimentation in the Pacific rim: International Association of Hydraulogical Sciences Publication 165, p. 27-38.

Dietrich, W.E., Wilson, C.J., and Reneau, S.L., 1986, Hollows, colluvium, and landslides in soil-mantled landscapes, in Abrahams, A.D., ed., Hillslope processes: The Binghamton Symposia in Geomorphology; International Series, no. 16, Allen and Unwin, Boston, 12 p.

Ellen, S.D., 1988, Description and mechanics of soil slip/debris flows in the storm, in Ellen, S.D., and Weiczorek, G.F., eds., Landslides, floods, and marine effects of the January 3-5, 1982, storm in the San Francisco Bay region, California: U.S. Geological Survey Professional Paper 1434, p. 63-112.

Ellen, S.D., and Fleming, R.W., 1987, Mobilization of debris flows from soil slips, San Francisco Bay region, California, in Costa, J.E., and Wieczorek, G.F., eds., Debris flows/avalanches: process, recognition, and mitigation: Geological Society of America Reviews in Engineering Geology, v. 12, p. 31-40.

Ellen, S.D., Peterson, D.M., and Reid, G.O., 1982, Map showing areas susceptible to different hazards from shallow landsliding, Marin County and adjacent parts of Sonoma County, California: U.S. Geological Survey Miscellaneous Field Studies Map MF-1406, scale 1:62,500.

Hack, J. T., 1965, Geomorphology of the Shenandoah Valley: U.S. Geological Survey Professional Paper 484, 84 p.

Hack, J. T., and Goodlett, J. C., 1960, Geomorphology and forest ecology of a mountain region in the central Appalachians: U.S. Geological Survey Professional Paper 347, 66 p.

Herd, D.G., and Brabb, E. E., 1980, Faults at the General Electric test reactor site, Vallecitos Nuclear Center, Pleasanton, California; A summary review of their geometry, age of last movement, recurrence, origin, and tectonic setting, and the age of the Livermore Gravels: U.S. Geological Survey Administrative Report, April, 1980, 77 p.

Isaacson, K.A., 1990, Late Tertiary synorogenic sedimentation in the northern Livermore basin, California, [M.S. thesis]: San Jose State University, San Jose, 104 p.

Iverson, R.M., and Major, J.J., 1986, Groundwater seepage vectors and the potential for hillslope failure and debris flow mobilization: Water Resources Research, v. 22, p. 1543-1548.

Johnson, A.M., 1970, Physical processes in geology: Freeman and Cooper, San Francisco, 577 p.

Johnson, D.L., 1977, The late Quaternary climate of coastal California: Evidence of an ice age refugium: Quaternary Research, v. 8, p. 154-179.

Kirkby, M.J., 1987, Modelling some influences of soil erosion, landslides, and valley gradient on drainage density and hollow development: Catena, Supplement 10, p. 1-14.

Ollenburger, R.D., 1986, Source and stratigraphy of the Livermore Gravels, Alameda County, California, [M.S. thesis]: California State University, Hayward, 218 p.

Page, B.M., 1982, The Calaveras fault zone of California - an active plate boundary element: California Division of Mines and Geology Special Publication 62, p. 175-197.

Pierson, T.C., 1980, Piezometric response to rainstorms in forested hillslope drainage depressions: Journal of Hydrology, v. 19, p. 1-10.

Rantz, S.E., 1971, Precipitation depth-duration-frequency relations for the San Francisco Bay region, California: U.S. Geological Survey Professional Paper 750-C, p. C237-C241.

Reid, M.E., Nielsen, H.P., and Dreiss, S.J., 1988, Hydrologic factors triggering a shallow hillslope failure: Association of Engineering Geologists Bulletin, v. 25, p. 349-361.

Reneau, S.L., 1988, Depositional and erosional history of hollows: Application to landslide location and frequency, long-term erosion rates, and the effects of climatic change [Ph.D Dissertation]: University of California, Berkeley, 328 p.

Reneau, S.L., and Dietrich, W.E., 1987, The importance of hollows in debris flow studies; examples from Marin County, California, in Costa, J.E., and Wieczorek, G.F., eds., Debris flows/avalanches; process, recognition, and mitigation: Geological Society of America Reviews in Engineering Geology, v. 12, p. 165-180.

Reneau, S.L., Dietrich, W.E., Wilson, C.J., and Rogers, J.D., 1984, Colluvial deposits and associated landslides in the northern San Francisco Bay Area, California, U.S.A.: International Society for Soil Mechanics and Foundation Engineering, 4th International Symposium on Landslides, Proceedings, Toronto, Ontario, Canada, p. 425-430.

Sidle, R.C., 1984, Shallow groundwater fluctuations in unstable slopes of coastal Alaska: Zietschrift fur Gletscherkunde und Glazialgeologie, v. 20, p. 79-95.

Sidle, R.C., 1986, Groundwater fluctuations in unstable slopes of coastal Alaska, in Conjunctive water use: IAHS International Association f Hydraulogical Sciences Publication 156, p. 335-343.

Strahler, A.N., 1964, Quantitative geomorphology of drainage basins and channel networks, in Chow, V.T., ed., Handbook of Applied Hydrology: McGraw-Hill, New York. 34 p.

Tsukamoto, Y., 1973, Study of the growth of a stream channel; relation between stream channel growth and landslides occurring during heavy storm: Shin-sabo, v. 25, p. 4-13.

Welch, L.E., and others, 1966, Soil survey of the Alameda area, California: U.S. Department of Agriculture, Soil Conservation Service, Soil Survey Series 1961, no. 41, 95 p., 42 sheets.

Wilson, C.J., and Dietrich, W.E., 1987, The contribution of bedrock groundwater flow to storm runoff and pore pressure development in hollows, in Beschta, R.L., Blinn, T., Grant, G.E., Ice, G.G., and Swanson, F.J., eds., Erosion and Sedimentation in the Pacific Rim: IAHS International Association of Hydraulogical Sciences Publication 165, p. 49-60.

APPENDIX I.

SOIL PROFILE DESCRIPTIONS

The following soil profiles were logged in hand-dug pits in a hollow and on adjacent spurs. The location of the hollow is shown on plate 1. The locations used in each description assume a view point looking directly into the hollow.

Profile BS1-Top

This soil is Positas gravelly loam, 2 to 20 percent slope. It is exposed on the uppermost portion of the hollow backslope where it meets the upland surface. The profile is very similar to soil exposed in a pit dug down into the upland surface 200 m to the south. The A horizon is 94 cm (37 in) thick, massive to granular sandy clay in the upper half, grading downward to subangular, blocky, silty clay. Few pebbles or cobbles are visible. The B_{t1} is 48 cm (19 in) thick, with massive silty clay in between many large clasts. This upper B horizon grades into a lower, B_{t2} with nearly 95 percent clasts with highly plastic clay, down to a depth of at least 203 cm (80 in). This lower B horizon most likely grades into a C_{ox} below, however the pit could not be excavated further.

Profile BS1-R1

This soil is Positas gravelly loam, 40 to 60 percent slope. It is exposed in a debris-flow scar in the upper right part of the hollow. The A horizon is dark brown, granular clayey sand 38 cm (15 in) thick. The lower 23 cm (9 in) of the A horizon is 70 percent clasts with very few clay films and a loose consistency. The B horizon is only 8 cm (3 in) thick, consisting of clast-free yellowish-brown granular silty clay with an abrupt boundary with the underlying horizons. The C_{ox} horizon is 98 percent pebbles and cobbles with a clay-coated sand matrix, and it extends to a depth of more than 107 cm (42 in). Individual sand grains feel sticky when wetted, but will not form a ball when squeezed.

Profile BS1-RC1

This profile is located below R1 in the hollow and was exposed in a shallow debris-flow scarp. The A horizon is a dark-yellowish-brown sandy clay, 31 cm (12 in) thick with over 70 percent pebbles and cobbles. A B_1 horizon 15 cm (6 in) thick is identified on the basis of increased clay coats, increased cobble content, and an increase in stickiness. A B_{2a} and a B_{2b} are yellowish-brown gravelly clays, with a combined thickness of over 152 cm (60 in). The horizons are over 90 percent cobbles. Clay content gradually increases with depth, with the soil becoming increasingly sticky, despite a general increase in sand content.

Profile BS1-RC2

This profile is located below RC1 and is exposed in a debris-flow scarp.

The A horizon is dark-yellowish-brown, coarse sandy clay 36 cm (14 in) thick, with 30 percent pebbles and cobbles. The B_1 and B_2 horizons are yellowish-brown gravelly clays to clayey gravels over 89 cm (35 in) thick, with high cobble content. Clay content increases gradually as in the other profiles, and the soil becomes increasingly sticky despite the presence of the coarse gravels.

Profile BS1-R2

This profile is to the right of RC2, dug into the lower inside portion of the right spur, at the top of an old debris-flow scar. The profile is similar to BS1-RC2 with an A-horizon thickness of 20 cm (8 in) and a depth of 51 cm (20 in) to the sticky, plastic clay and clast-rich layer.

Profile BS1-L1

This profile is high on the left sidewall of the hollow, at the same elevation as R1. The A horizon is a dark-brown silty clay 36 cm (14 in) thick, with a moderate amount of pebbles and cobbles. Few clay films and coats are visible on smaller grains. The B_1 and B_2 horizons are dark yellowish-brown to brown, very cobble-rich sandy clays and sand, exposed down to a depth of 122 cm (48 in). Amounts of clay films increase with depth, and lower sands have very sticky clay coats.

Profile BS1-L2

This profile is on the upper part of the left spur, at the same elevation as L1. The A_1 horizon is a dark-brown, clayey silt 15 cm (6 in) thick. Many cobbles and some pebbles are present, with few, sticky-clay coats. The A_2 is a dark-yellowish-brown clayey to gravelly silt 15 cm (6 in) thick. Clay coats and stickiness increase with depth. The B_{t1} and B_{t2} are light-yellowish-brown to brownish-yellow sandy clay with high percentages of cobbles. Sticky clay coats are increasingly common with depth. The profile was exposed to a depth of 102 cm (40 in) with no sign of a C horizon.

M
GEOMO
ALA

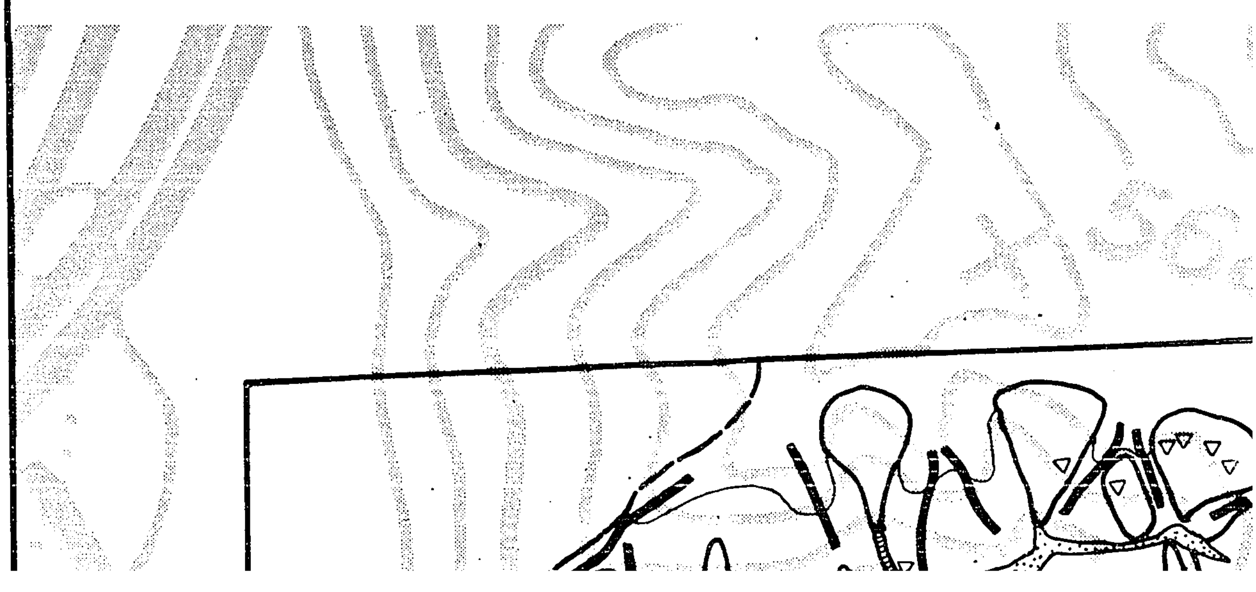

MAP SHOWING SELECTED
EOMORPHIC FEATURES NEAR SUN
ALAMEDA COUNTY, CALIFORNIA
BY
Christopher S. Alger
1991

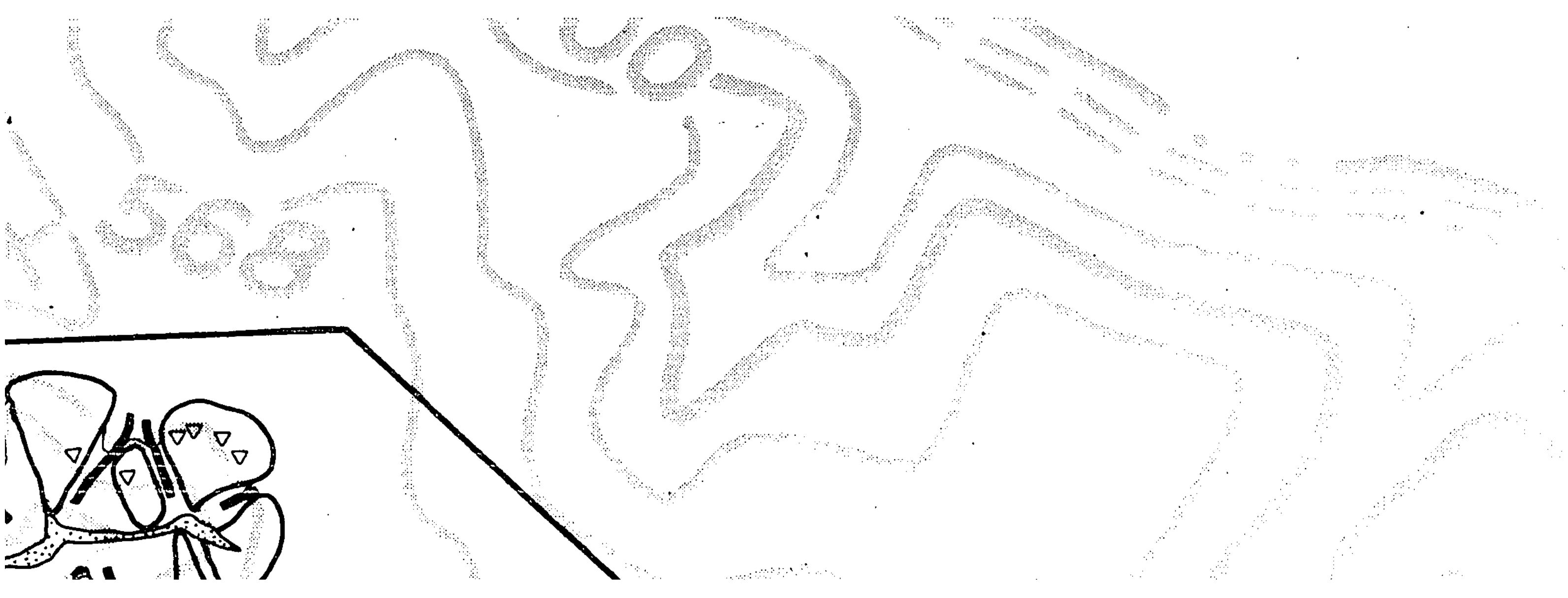

PLATE 1

ED
R SUNOL,
RNIA

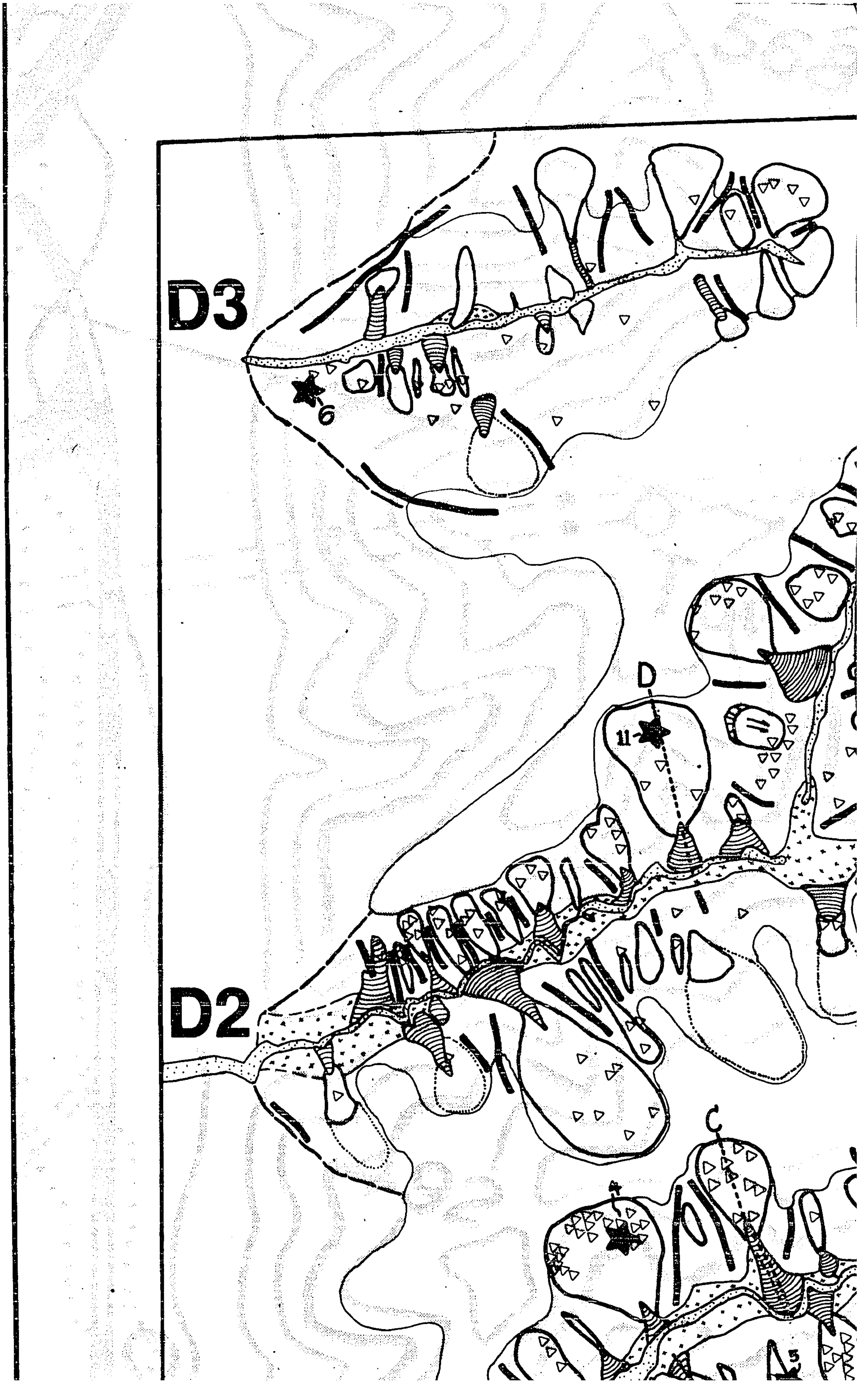

D3
D2
D
C
11
6
4
5

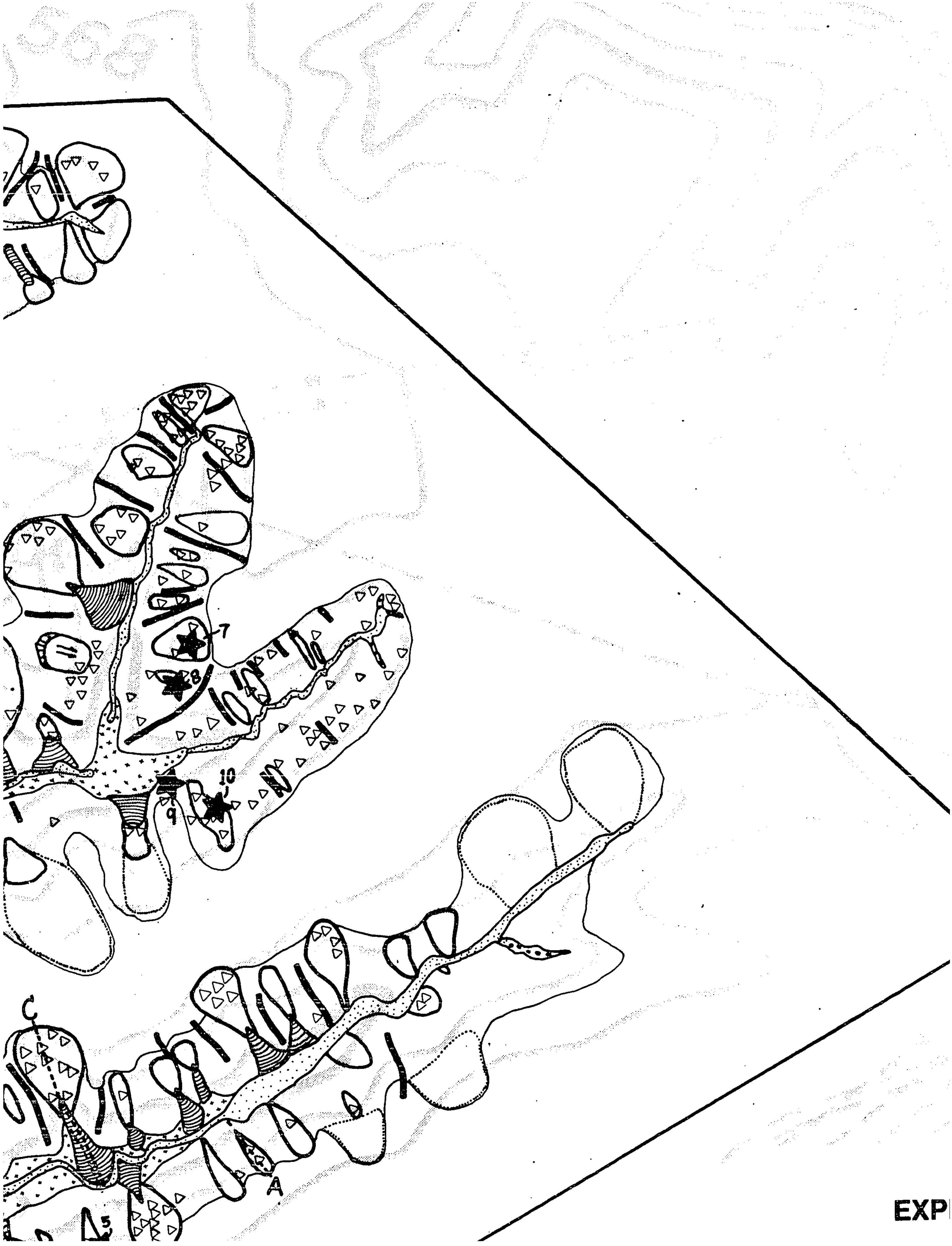

EXP

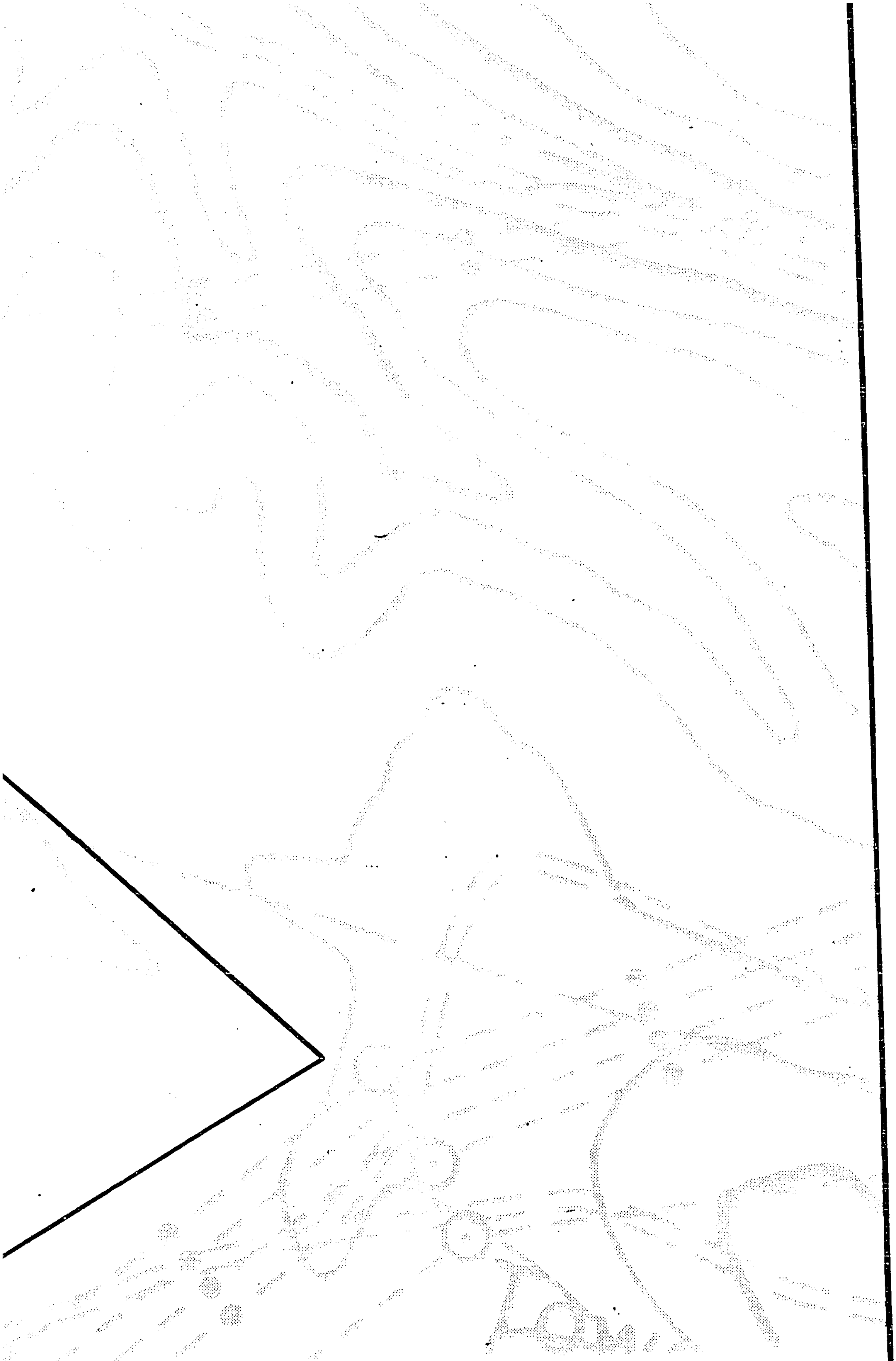

EXPLANATION

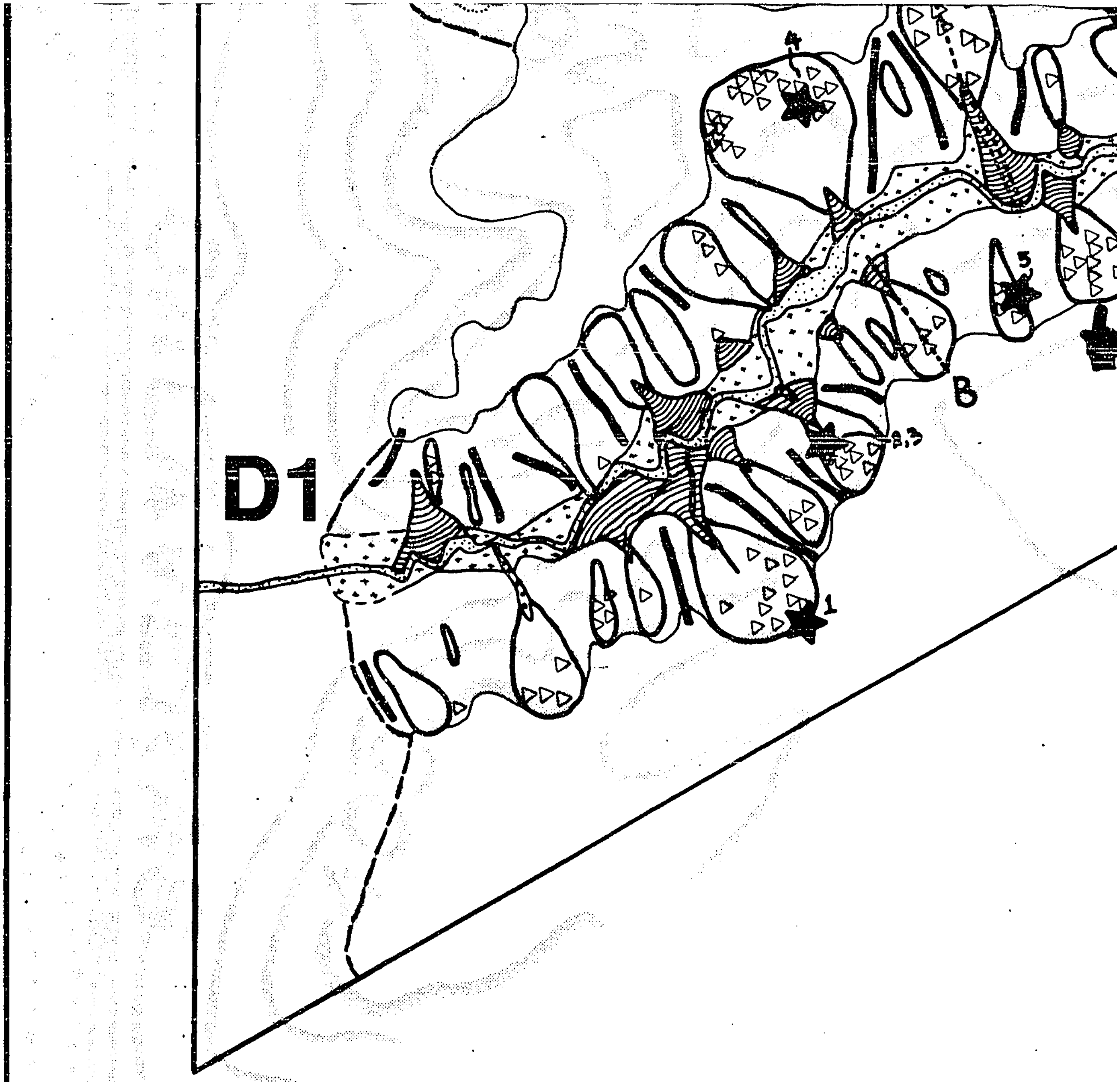

SCALE 1:3,000

0 250 500 750

0 100 200

CONTOUR INTERVAL 40 FEET

TOPOGRAPHIC BASE FROM U.S. GEOLOGICAL SURVEY
LA COSTA VALLEY QUADRANGLE, 1:24,000, 19

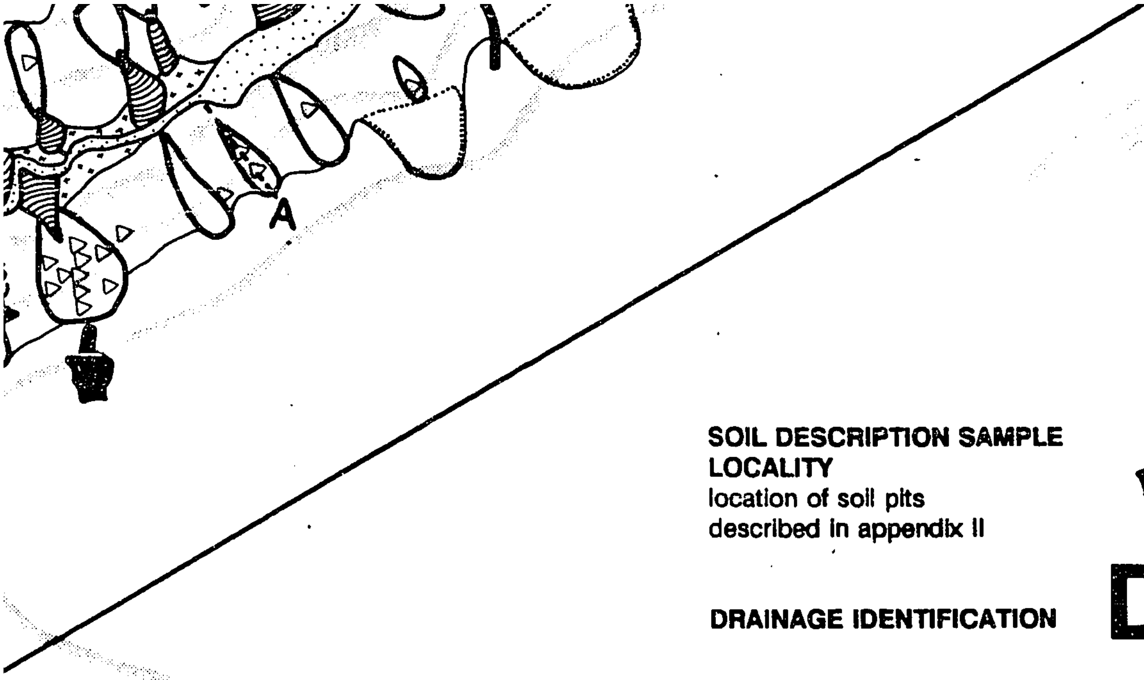

EXPLANATI(

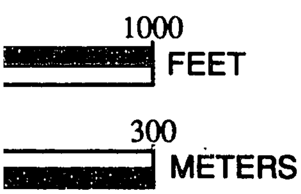

:T

SURVEY 7.5 MINUTE
4,000, 1969

SOIL DESCRIPTION SAMPLE LOCALITY
location of soil pits described in appendix II

DRAINAGE IDENTIFICATION **D1**

SOURCE OF DEBRIS FLOW
location of soil slip

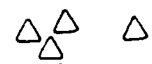

SOURCE OF DEBRIS FLOW TRIGGERED BY FEBRUARY, 1986 STORM
Location of soil slip triggered by the storm. Number corresponds to soil slip in tables and discussed in text

OLD COLLUVIUM
related to upland surface

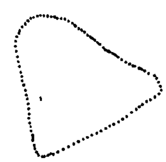

HOLLOW
hillside concavity

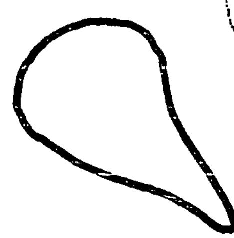

BOUNDARY OF MAPPED DRAINAGE

Mapped by the author June 1985 to June 1987.

BOUND/
remnant
surface

HILLSL(
located l
terrace c

LOCATI(
letter de:

SPUR R

FAN DE
gravel a
deposite
related p

INCISE
STREAI

GULLY
incised

TERRA(
colluvi
active c

EARTH
arrows

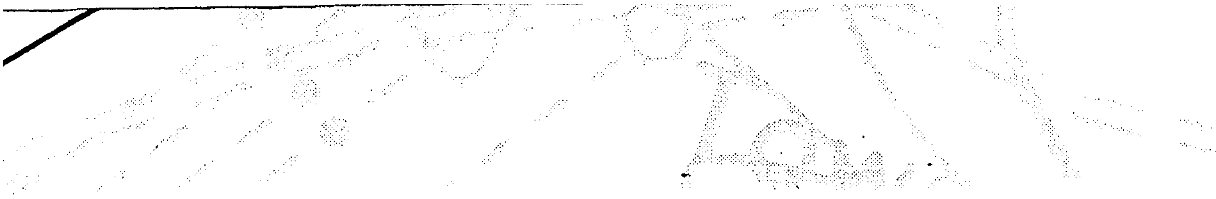

EXPLANATION

D1

6

ie
il slip

IAGE

1985 to June 1987.

BOUNDARY OF UPLAND SURFACE
remnant of old uplifted geomorphic surface

HILLSLOPE
located between upland surface and terrace deposits and/or fan deposits

LOCATION OF MEASURED PROFILE D
letter designates profile number

SPUR RIDGE

FAN DEPOSIT
gravel and fine-grained sediment deposited by primarily debris-flow related processes

INCISED CHANNEL OF ACTIVE STREAM

GULLY
incised into fan deposit

TERRACE DEPOSIT
colluvium and alluvium located between active channel and hillslopes

EARTH SLIDE
arrows indicate direction of movement